August 2012

Experimental & Empirical Correlations for the Determination of the Overall Volumetric Mass Transfer Coefficients of Carbon Dioxide in Stirred Tank Bioreactors

Syeda Anam Kazim
The University of Western Ontario

Supervisor
Dr. Amarjeet Bassi
The University of Western Ontario

Graduate Program in Chemical and Biochemical Engineering

A thesis submitted in partial fulfillment of the requirements for the degree in Master of Engineering Science

EXPERIMENTAL & EMPIRICAL CORRELATIONS FOR THE DETERMINATION OF THE OVERALL VOLUMETRIC MASS TRANSFER COEFFICIENTS OF CARBON DIOXIDE IN STIRRED TANK BIOREACTORS

(Thesis format: Monograph)

by

Syeda Anam Kazim

Graduate Program in Chemical & Biochemical Engineering

A thesis submitted in partial fulfillment
of the requirements for the degree of M.E.Sc in
Chemical & Biochemical Engineering

The School of Graduate and Postdoctoral Studies
The University of Western Ontario
London, Ontario, Canada

The University of Western Ontario
School of Graduate and Postdoctoral Studies

CERTIFICATE OF EXAMINATION

Supervisor

Dr. Amarjeet Bassi

Supervisory Committee

Dr. Mita Ray

Examiners

Dr. Mita Ray

Dr. Argyrios Margaritis

Dr. Anand Singh

The thesis by

Syeda Anam Kazim

entitled:

Experimental & Empirical Correlations for the Determination of the Overall Volumetric Mass Transfer Coefficient (K_La) of Carbon Dioxide in Stirred Tank Bioreactors

is accepted in partial fulfillment of the
requirements for the degree of
Biochemical & Biomaterials Engineering

Date

Chair of the Thesis Examination Board

Abstract

One of the most important parameters to cultivate microalgae is carbon dioxide absorption by microalgae. Therefore, it is necessary to determine the overall volumetric mass transfer coefficient (K_La) of carbon dioxide to quantify CO_2 transfer from the gaseous to the liquid phase. Until now, finding K_La of CO_2 for microalgae cultivation has been a challenge as there is not much information available about it in the literature and most of the time the CO_2 transfer to microalgae is approximated. In this study, correlations to directly calculate K_La of CO_2 in a stirred tank bioreactor are developed, and the combination of the parameters: 2000 ml/min, 350 rpm and 3% CO_2 content in air was found to be optimum for enhanced K_La of CO_2 in a stirred tank bioreactor.

Keywords: Overall volumetric mass transfer coefficient, Stirred tank bioreactor, Microalgae, Carbon dioxide, Correlations, Carbon dioxide probe

Dedication

I would like to dedicate this thesis

to my parents

Asad Kazim and Shaheen Asad

Acknowledgements

First, I would like to thank my supervisor Dr. Amarjeet Bassi for providing me his continuous support, guidance, and direction for this project. I have learnt valuable lessons under his tutelage on how to approach research and on the field of Biochemical Engineering as a whole. It has been an honour and pleasure working with him.

I would like to extend my thanks to my committee supervisor Dr. Mita Ray for her support and guidance to do well on my research work. I am also very grateful to Nadine Legros and Nanda Dimitrov from Teaching Support Centre for their continuous support and excellent workshops that made my journey of graduate school a joyous learning experience.

I am also thankfully acknowledging University Machine Services and Information Technology Service. I highly appreciate the assistance and valuable advice of Mr. Soheil Afara, Mr. Brian Dennis, Mr. Paul Sheller, Mr. Jesus Moreira and Mr. Stephen Mallinson throughout the time.

Special thanks go to my present and past lab mates in particular Ahmed Alasuity, Priyanka Saxena, Sanjay Kumar, Ana Maria Aguire, Claudia Sacasa Castellenos, Khalid Aribe, Teresa Turnbull, Juan Manuel, Ravi Balgobin, Charles, Gureet Chandhok, Harpreet Kaur and Shreyas Yedahalli. Without you all, my experience throughout my Master's study would not be nearly as colourful as it was. My most sincere thanks to my friends Aarica Arora, Samindika Athapathu, Baishakhi Dhar, Saeed Ahmed, Owais Khan, Faraz Shah, Shruti Srivastava and Hoi Ki Cheung. All of you consistently remind me to look for the silver lining in difficult situations.

Last but not least, I would like to express my deepest gratitude to my family members for believing the best in me. From you, I will always find an unwavering source of support to strive forward.

Table of Contents

List of Figures

List of Tables

Nomenclature

$[H_2CO_3]$	Concentration of H_2CO_3	g/L
b, c, d,e	Coefficient values for CO_2 used to relate solubility of CO_2 at different temperatures	Cal/mol k
a	Gas-liquid interfacial area per unit volume of fluid	m^3/m^2
A	Area across which mass transfer occurs	m^2
C_a	Concentration (of component A)	Kg/m^3
C_{A1}	Concentration of A in the bulk of the aqueous phase	Kg/m^3
C_{A1i}	Concentration of A at the interface of the aqueous phase	Kg/m^3
C_{A2}	Concentration of A in the bulk of the organic phase	Kg/m^3
C_{A2i}	Concentration of A at the interface of the bulk of the organic phase	Kg/m^3
C_{AG}	Concentration of A in bulk gas	Kg/m^3
C_{AGi}	Concentration of A at the interface in the gas phase	Kg/m^3
C_{AL}	Concentration of A in the liquid phase	Kg/m^3
C^*_{AL}	Saturated concentration of Component A in the liquid phase	Kg/m^3
C_{ALi}	Concentration of A at the interface in the liquid phase	Kg/m^3
C_o	Initial concentration of dissolved carbon dioxide at t_o	ppm
C^*	Saturated concentration of dissolved carbon dioxide	ppm
D	Diameter of impeller	m
D_{AB}	Binary diffusion coefficient for component A in the mixture of components A and B	m^2/s
D_{CO2}	Diffusion coefficient of CO_2 in water	m^2/s
Dec	Decarbonisation of flue gas	%
D_{eff}	Effective diffusion coefficient	m^2/s
$D_L^{CO_2}$	Diffusivity coefficient of carbon dioxide in liquid	m^2/s

$D_L^{O_2}$	Diffusivity coefficient of oxygen in liquid	m^2/s
D_t	Diameter of bioreactor	m
f_i	Gas fugacity of gas i	-
Flg	Gas flow number	-
Flgl, Flgu	Gas flow number for the lower and upper impeller respectively	-
Flg_{Avg}	Average of gas flow numbers for upper and lower impellers	-
Flg_{sum}	Sum of gas flow numbers for upper and lower impellers	-
Fr	Froude's number	-
g	Acceleration due to gravity	m/s^2
H	Henry's constant	atm.L/mol
H^{CO2}	Henry's constant for CO_2	$Pa.m^3/mol$
h	Gas hold up	-
J_A	Mass flux	$Kg/ m^{2/} s$
N_A	Rate of mass transfer (of component A)	Kg / s
N	Agitation rate of impeller inside reactor	rps (revolutions per second)
K_0, K_1, K_2	Equilibrium constants	L/g,g/L,g/L
K_{GA}	Overall gas absorption coefficient	m/s
K_L	Mass transfer coefficient	m/s
$K_L^{CO_2}$	Mass transfer coefficient of carbon dioxide	m/s
$K_L^{O_2}$	Mass transfer coefficient of oxygen	m/s
K_La	Liquid phase mass transfer coefficient coefficient	s^{-1}
m,n	Empirical coefficients relating partial pressure of CO_2 and pH of the system	-
Pr	Productivity	g/L/h
P	Power exerted by the impeller	Watts

P_{CO2}	Partial pressure of CO_2 in the air above the aqueous solution	atm
P_g	Power for aerated liquid	watts
P_L	Partial pressure of CO_2 at final point	atm
P_o	Partial pressure of CO_2 at initial point	atm
P_t	Total pressure at the liquid-gas interface	atm
Q_g	Flue gas flowrate	m^3/h
Q_i	Modified Henry's Law constant for gas i	atm.L/mol
R	Universal gas constant	cal K^{-1} mol^{-1}
Re	Reynold's number	-
T	Temperature	^oC, K
t	time	s
t_o	Initial time	s
U_g	Superficial velocity	m/s
U_{gs}	Superficial gas velocity	m/s
V	Volume	M^3
V_{CO2}	Aeration rate of CO_2 supplied to the microalgal culture medium	g CO_2/L/h
$\bar{v}_i$	Partial molal volume of gas i in solution	L
W	Width of impeller	m
X	Gas solubility	Mol/L
x_i	Mole fraction of gas i in solution	-
y	Distance	m
$\frac{dC_a}{dy}$	Concentration Gradient	$kg/m^3/s$

List of Abbreviations

DCW	Dried Cell Weight (g/L)
GC	Gas Chromatography
IRGA	Infra-Red Gas Analysis
ISE	Ion Selective Electrode
NDIR	non-dispersive infrared

Chapter 1: Introduction

1.1 Background:

Because of their unique properties and multiple applications, algae cultivation has become an important area of study for researchers and various industries. Both microalgae and macroalgae can be used to produce biodiesel and reduce pollution in wastewater facilities. In the latter case, wasterwater pollutants act as nutrients for algae. When algae grow they consume the contaminants and clean the water.

However, microalgae are more commonly used in comparison to macroalgae due to their extraordinary potential for cultivation as energy feedstock. Further, microalgae are unicellular unlike macroalgae, which are multi-cellular and because of this microalgae grow quickly even under difficult agro-climatic conditions. At present, seemingly, microalgae are the only source of biodiesel that can be produced in sufficient quantities to meet global demand. This is mainly due to the richness they have in oil content. In addition, they are used in bioreactors installed near power-plants to decrease carbon dioxide emissions from the plants. Moreover, algae are widely used in the cosmetic industry as an ingredient of the lipsticks and facial masks. (Chisti, 2007)

Microalgae production is mainly a photosynthetic growth requiring light, carbon dioxide, water and inorganic salts. They are usually cultivated either in open ponds (open system) or photobioreactors (closed system). Therefore, there are certain parameters that are considered carefully for microalgae growth, such as light intensity, temperature and growth medium. Moreover, experiments related to microalgae require the right choice of microalgae strain depending upon the purpose it will be used for. The selection is usually based on the oil content in the strain and the growth rate. *Chlorella sp*. is commonly used due to its high oil content and growth rate to run such experiments. (Chisti, 2007)

In addition, the design of a photobioreactor plays an important role in affecting the growth of microalgae. One of the main parameters of the design includes efficient transfer of carbon dioxide from the gaseous phase to the liquid phase. This is a crucial parameter as living cells (microalgae) consume only the dissolved carbon dioxide molecules, and carbon is one of the

essential nutrients for microalgae cultivation. Therefore, it is essential to design a photobioreator that operates at conditions that will allow maximum transfer of carbon dioxide. At the present time, in industrial production of microalgae, estimations for carbon dioxide feeding to a bioreactor are based on pH monitoring and dissolved oxygen measurements that only provide an approximation, and do not provide exact data about carbon dioxide consumption by microalgae.

The phenomenon of carbon dioxide transfer from the gaseous phase to the liquid phase is dependent on the overall mass transfer coefficient of carbon dioxide. The exact mass transfer coefficient values will help determine the transfer rate of gaseous carbon dioxide to a liquid phase, and the optimal amount of the gas supply needed to increase its consumption by microalgae for maximum possible growth. Therefore, the information about the overall mass transfer coefficient of carbon dioxide is essential for a better feeding control and accurate data of how much carbon dioxide has been consumed by microalgae in comparison to the supplied carbon dioxide.

1.2 Objectives:

The main purpose of the research was to investigate and determine the overall volumetric mass transfer coefficients (K_La) of carbon dioxide in a 10 L stirred tank bioreactor. The effect of the agitation rate and flowrate of air enriched with 3% CO_2 on $(K_La)_{CO2}$ was also investigated..

The specific objectives of the study included:

1) Analysis of the effect of change in agitation rate (rpm) on the K_La of CO_2.
2) Investigation of the relationship between the K_La and aeration rate
3) Determination of the conditions for enhanced K_La of CO_2 in stirred tank bioreactors
4) Development of correlations to directly calculate the overall volumetric mass transfer coefficient of carbon dioxide in stirred tank bioreactors operating at certain conditions.

1.3 Scope of the Thesis:

This thesis consists of five chapters. Chapter 1 provides background of the research topic and an introduction to the research study performed. Following chapter 1 is chapter 2 containing detailed literature review on solubility of carbon dioxide, dissolution of the gas in water, diffusivity and mass transfer of carbon dioxide, and overall volumetric mass transfer coefficient of the gas. In chapter 3, details about the materials and methods employed to conduct the research study on the measurement of the overall volumetric mass transfer coefficient of carbon dioxide are described. In chapter 4, all the results obtained are reported, analyzed and discussed. Chapter 5 is the last chapter that includes conclusions drawn from the experimental results and recommendations for future work.

Chapter 2: Literature Review

2.1 Introduction

Carbon dioxide is an omnipresent gas and is often produced from the oxidation reactions of organic compounds comprising carbon. These oxidation reactions can range from combustion of fuels to the metabolism of living organisms (Hill, 2006). The continuous increase in carbon dioxide emissions into the atmosphere have been regarded as major contributor to global warming (Kordac and Linek, 2008). For this reason, sequestration of carbon dioxide has become an important area of interest and many researchers are developing methods to capture or store this greenhouse gas.

Carbon dioxide is soluble in water and its solubility has been reported as being higher than other gases such as nitrogen, oxygen, argon, neon, krypton and helium (Weiss, 1974). In fact, the solubility of carbon dioxide is 26 times higher than oxygen (Kordac and Linek, 2008). For example, the solubility of carbon dioxide at standard ambient temperature and pressure in water is 1.5 ppm whereas; oxygen's solubility is 0.04 ppm(The Engineering Toolbox,). Due to carbon dioxide's high solubility in water, living organisms underwater consume carbon dioxide as it acts as a source of carbon for them. One such type of living cells is photosynthetic algae, which uptake carbon dioxide as food to supplement for the carbon nutrients (Hill, 2006).

Microalgae play a dual role to decrease the release of CO_2 into the atmosphere as they not only capture CO_2 but also produce biodiesel- a carbon neutral system. Therefore, production of biofuels from microalgae is another area of research that plays a key role in sequestrating CO_2.

Since algae absorb only dissolved carbon dioxide and diffusivity of carbon dioxide in water is 10,000 times slower than air, the rate of carbon dioxide absorption is a limiting factor for algae cultivation. The transfer rate of carbon dioxide is quantified by determining the volumetric mass transfer coefficient of carbon dioxide, which is an important parameter in photobioreactor design. Commonly, it is assumed that the mass transfer rate of carbon dioxide is equivalent to the mass transfer rate of oxygen. However, this assumption has been proven to be questionable as the mass transfer coefficients for carbon dioxide have been reported to be lower than the mass transfer coefficients for oxygen. (Hill, 2006;Johnson et al., 2010)

Several methods have been employed to measure the solubility and diffusivity of carbon dioxide in the aqueous phase. This is not the case for the mass transfer coefficient of carbon dioxide, where very few direct methods and correlations are reported. An understanding of the solubility and diffusivity of carbon dioxide is crucial to analyze the transfer rate of carbon dioxide from air bubbles into the aqueous phase, and determine the mass transfer coefficient of the gas. Therefore, in this chapter, details about the solubility and diffusivity of carbon dioxide are first discussed, methods to measure the concentration of dissolved carbon dioxide are next described, and finally correlations for the mass transfer coefficients of the gas as reported to this point will be discussed.

2.2 Solubility of Carbon Dioxide

The solubility of carbon dioxide in aqueous systems is a function of composition, temperature and pH. The solubility of CO_2 in sodium phosphate and 0.9% sodium chloride solutions is found to be lower than in water by 8%. This decrease in solubility of CO_2 in aqueous solutions is reported due to the electrolytes that hamper the gas making it less soluble. This effect is also referred to as “Salting out”. When the gas is dissolved in water, the gas molecules are surrounded by crystalline structure of water molecules. Similarly, in normal saline and phosphate buffer solutions, electrolytes surround the gas molecules and prevent the interaction between gas and water molecules. Hence, there is a decrease in the solubility of the gas in the saline and buffer solutions. (Yeh and Peterson, 1964)

Also, an inverse relationship between temperature and solubility has been explained due to the change in water crystallinity. At elevated temperatures, the crystalline structure of water molecules trapping the gas is broken. As a result, the water becomes less capable of capturing the gas molecules, thus the solubility of the gas is reduced at higher temperatures. (Yeh and Peterson, 1964)

The following correlation was developed to describe the dependence of the solubility of various gases on temperature. Therefore, the correlation can be used to predict the solubility of CO_2 at a certain temperature.

$$RlnX = b + cT^{-1} + dlnT + eT \quad (2.1)$$

Where, R is universal gas constant, X is gas solubility, T is temperature and b, c, d and e are the coefficients that depend on the type of gas; for CO_2 the coefficient values described in the table below:

Table 2.1:The Coefficient Values for Carbon Dioxide in Equation 2.1

(adapted from Wilhelm et al., 1977)

Gas	Temperature (K)	b (cal/mol K)	c (cal/mol)	d (cal/mol K)	e (cal/ mol K)
Carbon Dioxide	273-353	-317.658	17371.2	43.0607	-0.00219107

Moreover, the solubility of CO_2 varies with pH and the following correlations can be used to calculate the solubility of carbon dioxide at a certain pH.

$$[CO_2]_T = [CO_2] + \frac{K_1}{[10^{-pH}]} + \frac{K_1K_2}{[10^{-pH}]^2} \quad (2.2)$$

Where, K_1 and K_2 are equilibrium constants of the reactions and $[CO_2]_T$ is equal to

$$[CO_2]_T = [CO_2] + [CO_3^{-2}] + [HCO_3^-] + [H_2CO_3] \quad (2.3)$$

2.2.1 Measurement of the Solubility of Carbon Dioxide

The Microgasometric technique is one of the techniques to determine the solubility of carbon dioxide and was used by Weiss to measure the solubility of pure CO_2. The same technique was employed to measure the solubility of He and Ne and corrections for non-ideal gas behaviour were taken into account. The solubility of carbon dioxide was measured by fitting the data in the temperature and salinity equations developed originally for the gases, such as N_2, O_2, Ar, He, Ne and Kr. It was found that carbon dioxide is several times more soluble than N_2, O_2, Ar, He, Ne and Kr. (Weiss, 1974)

Further, it has been reported that in the gaseous form, the behaviour of carbon dioxide varies immensely from an ideal gas. Therefore, instead of the ideal gas approximation, Henry's law for real gases should be used and its validity to a wide spectrum of partial pressures of CO_2 should be checked. This will ensure accurate measurements for the solubility of carbon dioxide. In addition, Henry's coefficient varies with temperature and pressure, thus in order to measure the concentration of dissolved carbon dioxide at the interface, coefficient values specific to the conditions should be used. For this reason, a modified form of Henry's Law that takes into account the fugacity of CO_2 and total pressure of the system should be used to accurately measure the solubility of CO_2 in water. The modified form of Henry's Law for real gases is shown in the following equation.

$$f_i = Q_i x_i \exp(P\bar{v}_i/RT) \qquad (2.4)$$

where, f_i is the gas fugacity of gas i, x_i is the mole fraction of i in solution, $\bar{v}_i$ is the partial molal volume of i in solution, R is the gas constant, T is the absolute temperature, P is the total pressure at the liquid-gas interface, and Q_i is the modified Henry's Law constant for i, which is dependent merely on the temperature and the nature of the solvent. (Weiss, 1974)

Moreover, acidification is reported as an important factor to be considered while measuring the solubility of CO_2 in liquids. This is because acidification of liquids lowers the pH of the sample solutions and converts all of the bicarbonates, carbonates and carbonic acid into dissolved carbon dioxide as they are formed by the dissociation of dissolved hydrated CO_2 (shown in Equation 2.3). Consequently, the accurate measurement of dissolved carbon dioxide becomes possible by acidifying the solution. Therefore, when the solubility of CO_2 was measured in seawater by

Weiss (1974), the pH of the seawater was brought to very low values by adding sulphuric acid. The addition of sulphuric acid was reported to have a negligible impact on the salinity of seawater, thus the acid had no effect on the solubility of CO_2. (Weiss, 1974)

2.2.2 Diffusivity & Mass Transfer Rates

Diffusion occurs due to a concentration gradient. For example, molecules of component A will migrate, and there is a mass transfer of component A from the high concentration region to the low concentration region until the entire system is equilibrated. This process of migration and mass transfer because of concentration gradient is called diffusion.(Sherwood et al., 1975)

In order to quantify the diffusivity of various gases and liquids, diffusion coefficients are calculated. For instance, components with higher diffusion coefficient values diffuse more quickly than the components with lower diffusion coefficients. Moreover, diffusion coefficient values for a gas may vary depending upon the component it is mixed with. For example, diffusivity of carbon dioxide in water is different from the diffusivity of carbon dioxide in ethanol. Also, diffusivity of gases differs with changing temperatures and pressures. On the other hand, diffusivity values of liquids depend linearly on concentration and are several orders of magnitude smaller than the diffusivity values of gases.(Sherwood et al., 1975)

In the mixtures of two components, the diffusion coefficient of one of the components is usually referred to as the binary diffusion coefficient. For example, the diffusion coefficient of component A in the mixture of components A and B is denoted as D_{AB} and called the binary diffusion coefficient of A. (Doran, 1995)

The equation below is used to calculate the diffusivity of various components:

$$J_A = \frac{N_a}{A} = -D_{AB} \frac{dC_a}{dy} \quad (2.4)$$

J_A is the mass flux (rate of mass transfer per unit area perpendicular to the direction of movement) of component a, N_a is the rate of mass transfer of component A, A is the area across which mass transfer occurs, D_{AB} is the binary diffusion coefficient or diffusivity of component A in a mixture of A and B, C_a is the concentration of component A, y is distance, and $\frac{dC_a}{dy}$ is the concentration gradient (change in concentration of component A with distance). (Doran, 1995)

2.2.2.1 Natural Convection

Farajzadeh et al (2009) conducted an experiment in a cylindrical PVT (Pressure, Volume, Temperature) cell under the pressure range of 10-50 bars, and a specific volume of CO_2 was dissolved in a column of distilled water inside the cell. From the experiment, it was found that the mass transfer rate of carbon dioxide when dissolved in water is higher at the gas-liquid interface than predicted by Fickian diffusion and it escalates when the initial pressure of the gas is increased. This enhanced mass transfer rate of CO_2 has been explained as a result of natural convection, which takes place due to the destabilization of the gas-liquid interface caused by the increase in density of aqueous CO_2 after CO_2 is dissolved in water. In other words, the driving force for natural convection is developed when the water with CO_2 moves upwards to the interface and denser water with less CO_2 moves downwards thus accelerating the mass transfer rate. Furthermore, the change in density of aqueous CO_2 depends immensely on the CO_2 concentration (initial pressure of the gas) that is, the higher the concentration, the higher will be the increase in the density. (Farajzadeh et al., 2009)

However, diffusion takes place initially when CO_2 and water are brought in contact, but after some time natural convection begins to control the mass transfer once aqueous CO_2 becomes denser. Moreover, once natural convection is activated, enhanced mass transfer mitigates overtime and CO_2 dissolution continues mainly because of classical diffusion behaviour. At this point, the mass transfer rate is independent of the initial pressure of the gas. Thus, it can be seen how natural convection is triggered during the mass transfer of CO_2 into water, which is not taken into account by Fickian diffusion. For this reason, counting on Fickian diffusion solely to

determine the mass transfer rate of the gas may not give accurate results. (Farajzadeh et al., 2007;Farajzadeh et al., 2009)

2.2.2.2 Diffusion Coefficient of Carbon Dioxide in Water

Moreover, Farajzadeh et al (2007) performed another PVT cell experiment, which consisted of a gas column situated at the top of the liquid column. As the gas was dissolving in water there was reduction in pressure and that change in pressure was constantly measured over time. In this way, the mass transfer rate of CO_2 in water was measured inside PVT cell at the constant temperature of 25^{o}C and various initial pressures of CO_2. It was found from the experiment that the mass transfer of CO_2 in water at the interface is an unsteady diffusion process. (Farajzadeh et al., 2007)

In general, according to Fick's second law the diffusion coefficient of CO_2 in water has been reported as $D_{CO2} = 1.92 \times 10^{-9}$ m^2/s. On the contrary, Farajzadeh et al (2007) determined the effective diffusion coefficient by taking into account the phenomenon of natural convection as explained in Section 2.2.2.1 and reported the coefficient value as being one order of magnitude larger than the Fick's diffusion coefficient. The value of the effective diffusion coefficient as reported by Farajzadeh et al (2007) is $D_{eff} = 8.35 \times 10^{-8}$ m^2/s. Further, they reported a decrease in the effective diffusion coefficient once the effect of natural convection mitigated overtime and classical diffusion began to control the mass transfer of the gas into liquid. This decrease in the effective diffusion coefficient of carbon dioxide due to the mitigation of natural convection was expected because the effective diffusion coefficient is directly proportional to the natural convection. Later, the diffusion coefficient was measured again at the time the mass transfer was controlled by classical diffusion, and the coefficient was found to be closer to the values as mentioned in the literature for the diffusivity of CO_2 in water that is, $D_{eff} = 2.75 \times 10^{-9}$m^2/s. (Farajzadeh et al., 2007)

Farajzadeh et al. (2007) observed that as CO_2 was dissolving, in the beginning, the pressure of the gas was decreased drastically due to the enhanced mass transfer rate. But later on, there was a gradual decrease in the pressure as the diffusion process began to control the mass transfer. In addition, in the figure, the data from Fick's model was compared with the modified Fick's model with one effective diffusion coefficient, and it is evident that the mass transfer rate of CO_2 is higher than that predicted by Fick's model. Although the modified Fick's model with one effective diffusion coefficient takes into account natural convection, this model cannot be used to model the mass transfer process because of the mitigation of natural convection at the later stages of the mass transfer. Therefore, the mass transfer process of CO_2 can be modeled accurately by measuring two diffusion coefficients separately for each case that is, during the mass transfer controlled by natural convection and mass transfer controlled by classical diffusion. (Farajzadeh et al., 2007)

2.2.2.3 Diffusion of Carbon Dioxide in a Surfactant Solution

Furthermore, Farajzadeh et al (2007) analyzed the effect of a surfactant solution on the mass transfer rate of CO_2 in water. It was found that the addition of the surfactant sodium docedyl sulfate did not significantly change the transfer rate of CO_2 in water. In fact, when the salt sodium chloride (NaCl) was added to the surfactant solution, the mass transfer was impeded. This reduction in mass transfer can occur because of several reasons; first, the increase in viscosity due to the presence of salt, which prevents natural convection, thus decreases the effective diffusion coefficient; second, decrease in solubility of the gas after adding salt and this lessens the amount of CO_2 that is dissolved; and last, salt insertion leads to the adsorption of the surfactant molecules on the interface causing hindrance at the interface hence retarding the mass transfer. In short, addition of surfactant slows down the diffusion of CO_2 into water as the surfactant disrupts the mass transfer of the gas into the liquid. (Farajzadeh et al., 2007)

2.2.2.4 Carbon Dioxide Absorption in Carbonate & Alkaline Solutions

Payne & Dodge (1932) determined the absorption rates of carbon dioxide in water, sodium carbonate, sodium bicarbonate and sodium hydroxide solutions in a small tower packed with glass rings. The absorption rates were compared and reported in the form of an overall gas absorption coefficient K_Ga (grams absorbed per hour per cubic centimeter of packed volume per atmosphere of mean driving force).

According to Payne & Dodge (1932), considering only pure diffusional theory to explain carbon dioxide absorption in sodium carbonate and alkaline solutions is inadequate. Therefore, it is necessary to take into account both the pure diffusional theory and the chemical reaction rates of carbon dioxide in the solvent. The carbon dioxide absorption rates were reported by taking into account the following set of reactions:

$$CO_2(gas) \leftrightarrow CO_2(dissolved) \quad (2.5)$$

$$CO_2(dissolved) + H_2O \leftrightarrow H_2CO_3 \quad (2.6)$$

$$H_2CO_3 \leftrightarrow H^- + HCO_3^- \quad (2.7)$$

$$HCO_3^- \leftrightarrow H^+ + CO_3^{--} \quad (2.8)$$

$$H^+ + OH^- \leftrightarrow H_2O \quad (2.9)$$

$$CO_2 + OH^- \leftrightarrow HCO_3^- \quad (2.10)$$

$$HCO_3^- + OH^- \leftrightarrow CO_3^{--} + H_2O \quad (2.11)$$

$$CO_2 + 2OH^- \leftrightarrow CO_3^{--} + H_2O \quad (2.12)$$

(Payne and Dodge, 1932)

In alkaline solutions, higher absorption rates of CO_2 were noticed than water and carbonate solutions. Usually, reactions with ions are instantaneous, but for carbon dioxide absorption, Reactions 2.6, 2.10 and 2.12 are sluggish enough to affect the absorption rate. As a matter of fact, Reaction 2.6 has been reported as the limiting step reaction in the case of carbon dioxide absorption in alkaline solutions. Because of the slow reaction rates, the driving force across the interface becomes small, which reduces the absorption coefficient of CO_2. For this reason, lowest absorption coefficient of CO_2 was observed by Payne & Dodge (1932) particularly in a dilute sodium carbonate solution as compared to water and alkaline solutions. The reason for this observation is the excessive presence of carbonates in the case of the dilute sodium carbonate solution, which further slowed down the reaction between CO_2 and the solution. In the case of CO_2 absorption in sodium hydroxide (alkaline solution), the excessive quantity of OH^- ions made the presence of $HCO3^-$ ions negligible, and this caused the reaction in Equation 2.12 to occur rapidly. Hence, higher absorption coefficient values of CO_2 have been reported in alkaline solutions than water and carbonate solutions. (Payne and Dodge, 1932)

The absorption rate of CO_2 is temperature dependent. At higher temperatures, Eucken and Gr*ü*tzner (1927) observed higher absorption of carbon dioxide. The maximum absorption rates were reported in both pure water and alkaline solutions at the temperatures of 70^oC and 80^oC. Whereas, at a lower temperature such as 18^oC, the rate of overall reaction, which is the sum of Reactions 2.6 and 2.7, is found to be slow with the velocity constant of about 0.09 reciprocal seconds. Therefore, the CO_2 absorption reduces at low temperatures as the rates of the overall reaction become slower. (Eucken and Grutzner, 1927)

2.2.2.4.1 Dual-Film/Two-Film Theory of Mass Transfer

This theory models how mass transfer occurs when a solute moves from one phase to another phase. It states a fluid film or a mass transfer boundary is produced when two phases are brought in contact. Thus, in the case of mass transfer of a solute, the solute moves from the bulk of the first phase to the phase interface and then from the interface to the bulk of the second phase. (Treybal, 1968)

According to this theory, if a gas is highly soluble, then the gas film dominates and the absorption rate is dependent on the partial pressure of the solute in the gas: the higher the partial pressure of the solute in the gas, the higher will be the absorption rate. Carbon dioxide is considered to be a highly soluble gas and, therefore, it is expected to have gas-film controlling for carbon dioxide absorption in carbonate and alkaline solutions. In contrast, one of the experimental results for the carbon dioxide-air mixture absorption showed dependence of the CO_2 absorption coefficient on the solution's concentration. For example, Hatta (1929) analyzed the CO_2 absorption rate by sodium hydroxide and potassium hydroxide, and observed higher CO_2 absorption rates in potassium hydroxide than sodium hydroxide. This was mainly due to the higher concentration of OH^- ions in potassium hydroxide than sodium hydroxide as the dissociation constant of KOH is 0.5 and NaOH is 0.2 (Borkowski, 2005). Hence, Hatta (1929) explained the higher CO_2 observation in KOH using both diffusional and chemical kinetics theory. Therefore, it was concluded if chemical reactions are involved, as in the case of carbon dioxide, it is incorrect to predict the controlling film of resistance solely based on the solubility of the gas. (Hatta, 1929)

For this reason, a theory needed to be developed that could explain the absorption of carbon dioxide in detail in various types of solutions and take into account all the factors, such as

solubility, diffusion, chemical reactions and more factors that were not considered until then. Thus, determining the mass transfer coefficient of carbon dioxide became fundamental to explain the absorption of carbon dioxide. (Hatta, 1929)

2.3 Mass Transfer Coefficient (K_L) of Carbon Dioxide

Mass transfer of a component across an interface of the phases in contact is an important consideration because of the extremely slow fluid velocity at the interface. The two-film theory explains this decrease in velocity (as described in Section 2.2.2.4.1) as a consequence of no or very little turbulence in each fluid at the interface. Therefore, it is essential to determine the rate of mass transfer. (Treybal, 1968)

There are three cases of mass transfer: liquid-solid mass transfer, liquid-liquid mass transfer and gas-liquid mass transfer. In this work, gas-liquid mass transfer will be discussed to analyze the mass transfer coefficient of carbon dioxide in water.

The mass transfer of carbon dioxide from the gas phase to the liquid phase is expressed using the following equation:

$$N_a = K_L a(C^*_{AL} - C_{AL}) \quad (2.13)$$

Where N_a is the rate of carbon dioxide transfer per unit of time (gmol m^{-3} s^{-1}), K_L is the liquid phase mass transfer coefficient (m s^{-1}), a is the gas-liquid interfacial area per unit volume of fluid (m^2 m^{-3}), C_{AL} is the concentration of dissolved carbon dioxide in the broth, and C^*_{AL}, also called the solubility of carbon dioxide, is the saturated concentration of carbon dioxide in the broth (gmol m^{-3}). The concentration difference (C^*_{AL}- C_{AL}) refers to the driving force triggering mass transfer of carbon dioxide from the gas phase to the liquid phase. (Doran, 1995)

Since, carbon dioxide gas is not as highly soluble in water as ammonia and has a lower molecular diffusivity than oxygen; the mass transfer coefficient of CO_2 is either slightly lower or equivalent to oxygen. Therefore, the liquid-phase mass transfer resistance is controlling for the carbon dioxide mass transfer in the same way as oxygen mass transfer. This is contradictory to Payne & Dodge's (1932) observation, as they identified gas-film as the controlling factor in the case of carbon dioxide mass transfer in water. Thus, in Equation 2.10 K_La is considered as

liquid-film is assumed to be controlling. (Doran, 1995;Doucha et al., 2005;Kordac and Linek, 2008;Treybal, 1968)

Also, it is important to note that when there is a mass transfer of carbon dioxide from the gas phase to the liquid phase (water), out of all the dissolved species of carbon dioxide as shown in the set of equations in Section 2.2.2.4 only dissolved carbon dioxide is responsible for the carbon dioxide mass transfer through the gas-liquid interface. In fact, the concentration of dissolved CO_2 is three orders of magnitude more than carbonic acid (H_2CO_3). Therefore, when the mass transfer coefficient of CO_2 is determined the concentration of only dissolved carbon dioxide is taken into account. (Hill, 2006;Royce and Thornhill, 1991)

2.3.1 Overall Volumetric Mass Transfer Coefficient (K_La)

In the case of the mass transfer of a gas in which liquid-film resistance controls, the term overall volumetric mass transfer coefficient refers to the product of the mass transfer coefficient (K_L) and interfacial area a. It is generally very difficult to determine interfacial area 'a' because 'a' is dependent on bubble size and the number of bubbles, which are affected by other factors such as medium composition, agitation speed and gas flowrate. Therefore, the product of K_L and 'a' is measured through experiments or empirical correlations to quantify the mass transfer of a gas into liquid. (Andrew, 1982)

However, a method for mass transfer analysis in which both parameters are considered separately will better determine the dominant parameter controlling the mass transfer. (Singh and Majumder, 2010)

2.3.2 Carbon Dioxide Mass Transfer in Fermentation Broths

Generally, the mass transfer coefficient of carbon dioxide in water (non-fermentation broth) is usually reported as being lower than oxygen (Hill, 2006; Kordac and Linek, 2008). But, in fermentation broths the mass transfer coefficient of carbon dioxide has been reported as higher than the mass transfer coefficient of oxygen.

Usually, under the pH range of 4 to 8, the concentration of carbonate ions and reactions with hydroxyl ions are negligible, however the concentration of the bicarbonate ions increase as the pH is raised. Interestingly, in fermentation processes, the concentration of bicarbonate ions equalize with the concentration of carbon dioxide at a pH of approximately 6.3. As a result, Royce and Thornhill (1991) found the mass transfer coefficient of carbon dioxide to be 0.89 times higher than oxygen in the fermentation broth. Therefore, they developed an equation (as shown below) relating the ratio of the mass transfer coefficients of carbon dioxide and oxygen with the ratio of diffusivity coefficients of both gases in the liquid. (Hill, 2006;Kordac and Linek, 2008;Royce and Thornhill, 1991)

$$\frac{K_L{}^{CO_2}}{K_L^{O_2}} = \left(\frac{D_L^{CO_2}}{D_L^{O_2}}\right)^{2/3} = \left(\frac{2.0 \text{ X } 10^{-9} \text{ m}^2 \text{ s}^{-1}}{2.4 \text{ X } 10^{-9} \text{ m}^2 \text{ s}^{-1}}\right)^{2/3} = 0.89 \qquad (2.14)$$

(Royce and Thornhill, 1991)

Therefore, it can be concluded that there are variations in the way mass transfer of carbon dioxide occurs into the liquid phase when living cells are present in the system (fermentation broths) as compared to the systems with only water without the presence of cells in the system.

2.3.3 Factors Affecting the Overall Mass Transfer Coefficient (K_La) of Carbon Dioxide

There are several factors reported which affect the mass transfer coefficient of carbon dioxide and a few of them are discussed briefly as follows:

2.3.3.1 Superficial Gas Velocity

Higher values of overall mass transfer coefficient are obtained at higher gas velocities. An increase in superficial gas velocity causes an increase in gas holdup, which increases the interfacial area. There is an increase in interfacial area because higher gas velocity leads to higher momentum exchange between

phases. As a result, bubbles break at a higher efficiency into smaller bubbles and the interfacial area becomes bigger. (Singh and Majumder, 2010)

2.3.3.2 Surface Tension

The mass transfer coefficient is inversely proportional to the surface tension. Mass transfer for liquids with higher surface tension is lower because higher surface tension in liquids leads to the formation of bigger bubbles, which decreases gas hold up, thus lowering the overall volumetric mass transfer coefficient. Also, lower surface tension provides lower resistance stretching. However, adding surfactants to the solutions can help increase mass transfer coefficient as surfactants prevent bubbles coalescing and help to increase the interfacial area. (Singh and Majumder, 2010)

2.3.3.3 Viscosity

The mass transfer coefficient is higher in less viscous liquids. Liquids with lower viscosity have a lower resistance, which allows increased mass transfer from gas to liquid phase. When the liquid viscosity is high, there is a formation of larger bubbles, which decreases the overall gas hold up, thus the overall mass transfer coefficient. (Singh and Majumder, 2010)

2.3.3.4 Bubble Size

A slight change in bubble size does not affect the mass transfer. If the change in bubble size is big, then the mass transfer coefficient is changed significantly. Smaller bubble size leads to better mass transfer and increases the overall volumetric mass transfer coefficient. (Singh and Majumder, 2010)

In addition, it has been reported that the shape of gas bubbles during gas-liquid mass transfer is ellipsoidal instead of circular as mentioned in Higbie's classical penetration theory. For this reason, it is important to take into account the correction factors for ellipsoidal bubbles in correlations requiring bubble size to measure K_La. (Nedeltchev et al., 2006)

2.3.3.5 Gas Hold Up

It has been reported that as the mass transfer coefficient increases, gas hold up increases as well. Also, the factors influencing the mass transfer coefficient affect gas hold up in the same way. For example, an increase in gas velocity and decrease in surface tension increases gas hold up.

The effect of the above parameters on the mass transfer coefficient was explained by generating graphs in Matlab and through simulations for carbon dioxide mass transfer in the liquid phase inside a vertical bubble column. (Singh and Majumder, 2010)

2.3.3.6 Addition of Salt

Although the addition of salt reduces the rate of bubble coalescence, it does not significantly affect the mass transfer coefficient of carbon dioxide. In an experiment, mass transfer coefficients of carbon dioxide were measured in pure water and 2.85% salt solution (addition of sodium chloride (NaCl)) inside a stirred vessel. When the experimental data in both scenarios was compared, it was found that the mass transfer coefficient of CO_2 was insignificantly lower in salt solution than in pure water. Although the decrease in the mass transfer coefficient of CO_2 in a salt solution is very small it happens due to the hindrance caused by the salt molecules that prevents the mass transfer of CO_2 into the liquid phase. (Kordac and Linek, 2008)

2.4 Techniques to Measure Dissolved Carbon Dioxide

2.4.1 Direct Methods

2.4.1.1 Infra-Red Gas Analysis (IRGA)

One of the direct methods for measuring dissolved carbon dioxide is an in-situ method that uses an Infra-Red Gas Analysis (IRGA) sensor. This sensor is composed of a single beam dual wavelength non-dispersive infrared (NDIR) light source and a silicone based sensor covered with a CO_2 permissible polytetrafluoroethylene membrane. The carbon dioxide in the sample travels through the membrane inside the probe and absorbs photons from the NDIR light source. Once photons are absorbed, IRGA measures the wavelength of the beam based on the number of photons absorbed by the gas to quantify carbon dioxide present in the sample. When IRGA is connected to the transmitter, this measured wavelength by the IRGA sensor is then translated in the form of carbon dioxide partial pressure in the sample. The partial pressure obtained is then converted to the concentration of carbon dioxide using Henry's Law. This method was employed in various aquatic environments as it provides direct measurement of CO_2 concentration. (Johnson et al., 2010;St-Pierre, 2008)

The IRGA method has been reported as robust, accurate and responsive as the sensor's accuracy is ±1.5% for calibration range and 2% for reading. Further, no drift was observed in the probe's

reading even after using the sensor for more than six months. (Johnson et al., 2010)

2.4.1.2 Headspace Method

The Headspace Method is also reported as one of the best direct methods for measuring dissolved carbon dioxide. In this method, a water sample containing CO_2 is equilibrated with air and collected in an airtight syringe with a set headspace ratio. The sample is then analyzed using gas chromatography (GC) and concentrations of dissolved CO_2 are determined using Henry's Law.

2.4.1.2.1 Gas Chromatography

In Gas Chromatography, the sample collected in the airtight syringe is first heated to vaporize compounds present in the sample. A carrier gas pushes the vaporized compounds through a column with a solid substance inside, also called a stationary phase. The components of the sample are separated inside the column and they leave the column in sequence based on their affinity with the stationary phase. For example, the components having lower affinity with the stationary phase will leave the column before the components having higher affinity. The amount of time the peak requires to appear (retention time) identifies the component and the area of the peak (area below the curve) determines the concentration of the component.

The results obtained from the IRGA method and Direct Headspace Method were significantly different for some samples but were insignificantly different for other samples. (Johnson, et.al., 2009)

2.4.1.2 Henry's Law

The Henry's Law equation below can be used to determine the concentration of dissolved carbon dioxide from the partial pressure of carbon dioxide in a sample.

$$P_{CO_2} = H * [H_2CO_3] \tag{2.15}$$

Where, P_{CO_2} is the partial pressure of carbon dioxide in the air above the aqueous solution (atm), H is Henry's constant of carbon dioxide (atm.L/mol), $[H_2CO_3]$ is the dissolved concentration of carbonic ions, which takes into account both dissolved CO_2 and H_2CO_3 in the aqueous phase (mol/L). (Hill, 2006)

Henry's constant is a function of temperature. It changes as the temperature of the sample changes. For this reason, it is crucial to calculate Henry's coefficient at a specific temperature. The equation below can be used to generate Henry's coefficients of carbon dioxide at various temperatures.

$$H^{CO_2} = exp\left\{11.25 - \frac{395.9}{(T - 175.9)}\right\} \quad (2.16)$$

Where $H^{CO_2}$is Henry's coefficient in Pa.m^3/mol, and T is temperature of broth in Kelvin (K). (Royce and Thornhill, 1991)

2.4.2 Indirect Methods

2.4.2.1 Indirect Headspace Method

In the Indirect Headspace Method, 5 ml of stream-water is injected through a sterile syringe into a glass sealed vial, which was initially filled with 0.5 ml of 0.6% hydrochloric acid (HCl) and nitrogen (N_2) at atmospheric pressure. Hydrochloric acid is added to acidify the sample so that all the inorganic compounds of dissolved carbon dioxide are transformed into CO_2. After this conversion, dissolved CO_2 is then determined using gas chromatography (GC) and the concentration of dissolved carbon dioxide is figured from the temperature and pH dependent equilibria. (Johnson et al., 2010)

The results for fresh water aquatic systems obtained from indirect headspace and IRGA sensor methods were very similar. However, the sensor is able to give accurate results in both well-mixed and poorly mixed water systems. Whereas, the "headspace syringe sampling disturbs natural concentration profiles". (Johnson et al., 2010)

Up until now, researchers have been limited to two methods for measuring dissolved carbon dioxide in fresh water systems:

1) Immediate examination of a headspace equilibrated with water to measure dissolved carbon dioxide as soon as the sample is collected.
2) Indirect estimation of the concentration of dissolved carbon dioxide based on the calculations of pH and alkalinity

(St-Pierre, 2008)

2.4.2.2 pH Probe Method

Using a pH probe to measure volumetric mass transfer coefficient of carbon dioxide in a well mixed reactor is one of the indirect dynamic methods that has been employed by a number of researchers. The pH values vary as the sample solution acidifies due to carbon dioxide absorption. These values are recorded to generate correlations and estimate the mass transfer coefficient of carbon dioxide in the solution.

In this method, three main chemical reactions, as shown below, are considered that occur when carbon dioxide dissolves in water.

$$H_2O + CO_2 \overset{K_0}{\leftrightarrow} H_2CO_3 \quad (2.17)$$

$$H_2CO_3 \overset{K_1}{\leftrightarrow} H^+ + HCO_3^- \quad (2.18)$$

$$HCO_3^- \overset{K_2}{\leftrightarrow} H^+ + CO_3^{-2} \quad (2.19)$$

The equilibrium constants of the above reactions are determined. Reactions 2.18 and 2.19 are reported as being much faster as compared to Reaction 2.17; therefore, Reaction 2.17 is referred to as the rate limiting reaction. Once the equilibrium constants are calculated, concentrations of the carbonate and bicarbonate species are determined by the solving the following five equations:

$$[H_2CO_3] = \frac{[H^+][HCO_3^-]}{K_1} \quad (2.20)$$

$$[HCO_3^-] = \frac{[H^+][CO_3^{-2}]}{K_2} \quad (2.21)$$

$$[H^+] = \frac{1\ x\ 10^{-14}}{[OH^-]} \quad (2.22)$$

$$P_{CO_2} = H * [H_2CO_3] \quad (2.23)$$

$$[H^+] = [OH^-] + [HCO_3^-] + 2[CO_3^{-2}] \quad (2.24)$$

The determined concentrations of the species are used to develop correlations to calculate the volumetric mass transfer coefficient of carbon dioxide. (Hill, 2006)

This method is very time consuming as it requires many calculations even after the correlation is developed and gives only an estimation of volumetric mass transfer coefficient of carbon dioxide.

All in all, the use of sensors to measure dissolved carbon dioxide is reported as the most reliable method because sensors are capable of detecting the small-scale changes in the CO_2 concentrations unlike the methods requiring pH measurements to determine CO_2 concentrations. (Johnson et al., 2010)

2.4.3 A Comparison of the Probes Used in Fermentation Broths to Measure Dissolved Carbon Dioxide

For fermentation of *Streptomyces fradiae* in an oil based medium in an agitated vessel, the following probes were used to measure dissolved carbon dioxide. Their performances are compared in the table below:

Table 2.2:Types of Probes to Measure Dissolved Carbon Dioxide in Fermentation Broths

(adpated from Alford Jr, 1976)

Probe	Method Type	Description	Benefits	Limitations
Silastic Rubber Tubing	Indirect	1) 50 ft long silastic rubber tubing, permissible to CO_2 transfer with a nitrogen stream inside (0.2 ft^3/hr) was used to measure dissolved carbon dioxide. 2) The silastic rubber tubing was coiled around the air sparger near the bottom of the broth line. The outlet of the tubing was connected to an infrared analyzer	1) Inert to most substances 2) No Leaching out due to the addition of additives or plasticizers 3) Neither oxidizes or hardens with age 4) Easy to clean 5) Withstands repeated sterilization without altering its shape, strength and flexibility	1) Measures partial pressure of exhaust CO_2 gas instead of dissolved CO_2. 2) Sensitive to oily media and high solids. For example, oils of uninoculated *Streptomyces* media when covered the surface of the tubing reduced the efficiency of CO_2 transfer

		via stainless steel tubing to measure exhaust CO_2.	6) Non-wetting silicone-elastomer surface prevents sticking thus facilitating mass transfer 7) No impact of changes in medium temperature, pH, agitation, aeration, bicarbonate ion concentration and sterilization procedures	by 80%. 3) Unsuitable for on-line continuous dissolved CO2 measurements in fermentation processes. 4) Partial pressure of CO2 in a fermentor exhaust gas provides a good measure of the partial pressure of dissolved carbon dioxide in the liquid medium.
P_{CO2} electrode	Direct	1) Connected to pH meter to measure partial pressure of dissolved CO_2.	1) Measures partial pressure of dissolved CO_2.	1) Teflon membranes on the electrode couldn't withstand turbulence. 2) Thick membranes gave sluggish responses.
Thin walled Teflon tubing	Indirect	1) The tubing was installed in the same way as Silastic Rubber Tubing.	n/a	1) CO_2 transfer rate across the tubing is 81 times slower than Silastic Rubber Tubing. 2) Measures partial pressure of the exit CO_2.

2.5 Carbon Dioxide Absorption by Microalgae:

Carbon dioxide is the only carbon source for photosynthetic microalgae cultivation. When microalgae absorb CO_2, they not only fix CO_2 but also grow in numbers yielding products such as carotenoids, pigments, proteins, and vitamins that are utilized to make nutraceuticals, pharmaceuticals, animal feed additives and cosmetics. Moreover, microalgae form carbohydrates and lipids to produce energy, chemicals and foods upon consumption of CO_2. In fact, they have been reported as the only source of biodiesel that can produce biodiesel in quantities meeting global demand (Chisti, 2007). For this reason, it is necessary to have enhanced dissolution of CO_2 to prevent carbon limitation, which may occur due to the release of non-dissolved CO_2 out of the system. (Ryu et al., 2009)

There are several parameters that are usually taken into account for microalgae cultivation in a photobioreactor. In this work, the percentage content of CO_2 in air, aeration rate, and mass transfer coefficient of CO_2 in microalgal solution will be discussed.

Ryu et.al (2009) analyzed the impact of aeration rate, CO_2 concentration and bubble size on carbon dioxide absorption by *Chlorella sp.* in vertical tubular reactors without controlling the temperature of the system. According to their findings, a maximum cell concentration of 2.02 g/l was found at 5% CO_2 and the minimum cell concentration of 1.16 g/l was found at 0.5% CO_2 mixed in air. They suggested keeping the CO_2 concentration lower than 5% because higher CO_2 concentrations may inhibit microalgal growth. Furthermore, they reported a gradual increase in the cell concentration as the CO_2 concentration was increased. Therefore, it was concluded that CO_2 concentration is directly related to the cell concentration. However, changes in the CO_2 concentration do not play a significant role to drastically influence CO_2 fixation and there was a slight change in the fixation rate when the CO_2 content (%) was changed.

Moreover, an increase in the cultivation of *chlorella sp.* was observed as the aeration rate was increased. Therefore, it can be concluded that the aeration rate is directly proportional to the dried cell weight (DCW) of microalgae. On the other hand, there was a decrease in the CO_2 utilization efficiency upon increasing the aeration rate. In fact, above 0.20 vvm lesser increase in productivity was observed. Thus, the aeration rate should be optimized to ensure not only high

productivity but also high CO_2 utilization efficiency for economical large-scale productions. As in this case, 0.20 vvm is reported as the optimum aeration rate because a 1.3 fold increase in the productivity of *Chlorella sp.* was noticed when the aeration rate was raised from 0.10 to 0.20vvm. (Ryu et al., 2009)

CO_2 utilization efficiency was determined by using the following equation:

$$\text{CO2 utilization efficiency (\%)} = 0.57 \text{ x P x } \frac{\left(\frac{44}{12}\right)}{V_{CO_2}} \text{ x } 100 \qquad (2.25)$$

Where, 0.57 is the carbon content of the dried cell (g carbon/g biomass), P is the productivity (g biomass/L/h), 44 and 12 are the molecular weights of carbon dioxide and carbon, respectively, and V_{CO_2} is the aeration rate of CO_2 supplied to the microalgal culture medium (g CO_2/L/h). (Ryu et al., 2009)

For details about the effect of bubble size on microalgae cultivation please refer to the research paper of Ryu, et.al.

2.5.1 Flue Gas as a Source of Carbon Dioxide for Microalgae Cultivation

Flue gas that is released from power plants is often used as a source of carbon for microalgae cultivation. In fact, in Hawaii, algae are cultivated on a commercial-scale using flue gas from a power plant as a carbon source. Flue gas combusted from natural gas and containing 6 to 8% of carbon dioxide was used in one of the experiments by Doucha et al (2005) to grow *Chlorella sp*. in a photobioreactor with an area of 55m^2. It has been reported that *Chlorella sp*. could absorb 10 to 15% of carbon dioxide from the flue gas. However, at a higher flowrate, gas bubbles coalesce causing a reduction in CO_2 absorption by microalgae. Therefore, maximum CO_2 absorption was noticed at the lowest flue gas rate this occurrence. (Doucha et al., 2005)

Doucha et al. (2005) proposed a correlation to relate decarbonization of flue gas and flue gas flowrate was, which is as follows:

$$Dec = 100(1 - 0.282{Q_g}^{0.336}) \qquad (2.26)$$

Where, Dec (%) is decarbonisation of flue gas and Q_g is the flue gas flowrate (m^3/h)

(Doucha, Straka & Livansky, 2005)

Although microalgae absorbed 10% of NO_x from the flue gas, the gases such as NO_x and CO, at concentrations of up to 45mg/m^3 and 3mg/m^3 respectively showed no detrimental impact on microalgae cultivation. Also, inhibition in microalgal growth was prevented by keeping the partial pressure of dissolved carbon dioxide at least 0.1-0.2 kpa, because this pressure range minimizes the escape of CO_2 from the suspension. (Doucha et al., 2005)

The figure below shows the mass balance of CO_2 inside a photobioreactor when flue gas containing 8% CO_2 is supplied to the microalgae.

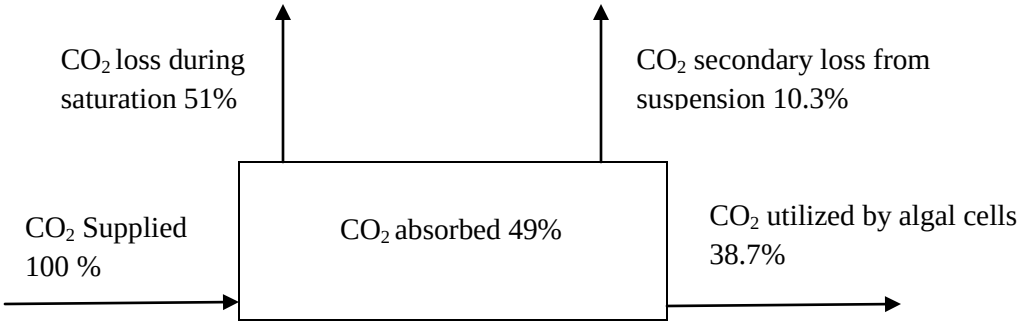

Figure 2.1: Carbon Dioxide Mass Balance in a Photobioreactor

(Doucha et al., 2005)

It has been reported that absorption of 49% CO_2 from flue gas means 4.4 kg of CO_2 is required to grow 1 kg of algal biomass. Thus, 470 kg of CO_2 in flue gas is adequate to produce 106 kg (dyr weight) of biomass per day. In this way, microalgae cultivation using CO_2 from flue gas can be very beneficial as it serves multiple purposes. For example, it helps reduce CO_2 emissions significantly through decarbonization of flue gas. Also, utilization of CO_2 in flue gas lowers the cost of the microalgae cultivation process by 15%. Moreover, a high density algal biomass will be available that can be used directly without the need for separation and drying to prepare animal feed. (Doucha et al., 2005)

2.5.2 Overall Volmetric Mass Transfer Coefficient of CO_2 in a Microalgal Solution

The mass transfer of carbon dioxide from a gas bubble to a microalgal cell occurs usually in the following seven steps:

1) There is bulk gas phase inside the bubble
2) The gas travels to the gas-liquid interphase
3) It crosses the liquid film around the bubble
4) The gas enters the bulk liquid culture medium
5) It passes through the liquid film around the microbial cells
6) The gas reaches the cell-liquid interface
7) Eventually, the gas crosses the intracellular gas transfer resistance

It is important to note that the liquid film around the bubble causes most of the resistance for the transfer of gas from the gas phase to the liquid phase. Whereas, the liquid film around the microbial cells is negligible due to the extremely small size of the cell and thus, does not contribute to cause any resistance. (Doran, 1995)

2.5.2.1 Impact of Culture pH on the Overall Volumetric Mass Transfer Coefficient of CO_2

In the experiment as explained in Section 2.5.1, the partial pressure of dissolved carbon dioxide was measured and the changes in the K_La of CO_2 with the change in culture pH were analyzed. A pCO_2 ion selective electrode (OP, 9353, RADELKIS, Budapest) connected to a pH meter was used to measure the partial pressure of dissolved carbon dioxide.

An exponential decrease was observed between the partial pressures P_o and P_L of dissolved CO_2 from the initial point to the final point respectively inside the photobioreactor. Therefore, the mean partial pressure of CO_2 was considered and calculated using the following equation:

$$P_{mean} = \frac{P_o - P_L}{\ln(P_o/P_L)} \tag{2.27}$$

The relationship between the partial pressure of CO_2 and pH of the system was analyzed by plotting $\log P_{CO_2}$ vs. pH of the system containing algal cells, and $\log P_{CO_2}$ was calculated by using Equation 2.28.

$$\log P_{CO_2} = m - npH \tag{2.28}$$

Where m and n are empirical coefficients that were experimentally determined and have the values of 8.434 and 1.201 respectively. (Doucha et al., 2005)

Doucha et al. (2005) observed a decrease in the partial pressure of carbon dioxide as the pH of the system containing microalgal cells was increased. Since the partial pressure of CO_2 decreases as the culture pH increases, the volumetric mass transfer coefficient of CO_2 lowers as well at higher pH conditions (Livansky, 1993).

The mass transfer coefficient of carbon dioxide was determined in the algal suspension using Equation 2.29, which is similar to the equation as reported by Royce and Thornhill (1991) in Section 2.3.2 to determine the mass transfer of CO_2 in a fermentation broth.

$$\frac{K_L{}^{CO_2}}{K_L^{O_2}} = \left(\frac{D_L^{CO_2}}{D_L^{O_2}}\right)^{1/2} \tag{2.29}$$

(Doucha et al., 2005)

The same equation as above was used in an experiment conducted by Babcock et al (2002) to determine the overall mass transfer coefficient of carbon dioxide in tap water, sea water and algal culture medium inside a near horizontal tubular reactor. But, the mass transfer coefficients of O_2 and CO_2 in Equation 2.29 were replaced with the volumetric mass transfer coefficients of the gases, and the equation was simplified as:

$$(K_L a)_{CO_2} = 0.90(K_L a)_{O_2} \tag{2.30}$$

(Babcock et al., 2002)

The overall mass transfer coefficient of CO_2 was calculated by first measuring the overall mass transfer coefficient of O_2 experimentally (for more details on the method employed to determine $(K_L a)_{O_2}$ please refer to the paper of Babcock et al.). Thus, indirect methods based on the overall mass transfer coefficient of oxygen were mostly employed that provided only an estimation of the overall mass transfer coefficient of carbon dioxide.

Until now, the methods and correlations that had been discussed in this section provided an approximation of the consumption of CO_2 by algal cultures on the basis of estimated K_La. However, it is necessary to quantify the CO_2 absorption by microalgae by determining the uptake rate of CO_2 by algal culture under different operating conditions to optimize photobioreactors' design. This requires the need of an efficient method that provides K_La of CO_2 directly and accurately so that the uptake rate by microalgae can be calculated.

Chapter 3: Materials & Methods

3.1 Materials & Chemicals:

Reagent grade Sodium bicarbonate (VWR, Mississauga, ON) was used to prepare the carbon dioxide standard solution (1000 ppm as CO_2). Reagent (GR) grade sodium citrate dihydrate (VWR, Mississauga, ON) and reagent grade concentrated hydrochloric acid (VWR, Mississauga, ON) were required to prepare the buffer solution. Carbon dioxide standard (1000 ppm as CO_2) and the buffer solutions were needed to calibrate the carbon dioxide ion selective electrode (Model no: ISE-8750, Omega, Laval, Quebec). Reagent grade sodium chloride (VWR, Mississauga, ON) was used to make a 0.1M sodium chloride solution as it was used to store the carbon dioxide ion selective electrode. Medical grade 99% pure carbon dioxide gas (Praxair, Mississauga, ON) was used to bubble the gas in the bioreactor, and medical grade 99% pure nitrogen gas (Praxair, Mississauga, ON) was used to push carbon dioxide gas out of the system. Reagent grade standard buffer solutions of pH 4 and 7 (VWR, Mississauga, ON) were needed to calibrate the Broadley James in-gel pH electrode (Eppendorf New Brunswick, Mississauga, ON) of the bioreactor. The ingold polarographic dissolved oxygen (DO) probe of the bioreactor (Eppendorf New Brunswick, Mississauga, ON) required a refill solution to prevent the inside of the electrode from drying.

3.2 Preparation of Solutions:

A 1L of **0.1M sodium bicarbonate ($NaHCO_3$) solution** was prepared by weighing 8.4 grams of reagent grade sodium bicarbonate in distilled water. Once the solution was prepared, 227 ml of it was diluted with distilled water to prepare 1L of standard **carbon dioxide solution** having the concentration of 1000 ppm as CO_2. In order to prepare 1L of the **buffer solution,** 294 grams of sodium citrate dihydrate ($NaC_6H_5O_7.2H_2O$) was poured in about 600 ml of water and the pH of the solution was adjusted to 4.5 adding hydrochloric acid to the solution. The final volume of the buffer solution was brought to 1L with additional distilled water. A 1L of **0.1M sodium chloride solution** was made by dissolving 5.8 grams of sodium chloride in distilled water.

.

3.3 Techniques Used to Measure Dissolved Carbon Dioxide:

In this section, the techniques that were employed to measure dissolved carbon dioxide in the buffer solution inside the bioreactor are discussed. A carbon dioxide probe was used to determine the concentration of dissolved carbon dioxide. Both the carbon dioxide probe and the bioreactor were interfaced with the computer to record all the data on timely basis. Therefore, details about the carbon dioxide probe and setup interface of the equipment with the computer are explained below:

3.3.1 Operation of the Ion Selective Carbon Dioxide Electrode:

The electrode was an ion-selective type based on the Severinghaus Principle. The probe had a membrane that allowed the passage of only dissolved carbon dioxide. When dissolved carbon dioxide passed through the membrane, it entered the probe in the form of carbonic acid (H_2CO_3), which brought a change in the H^+ ion concentration in the refill solution of the electrode. This change in the H^+ ion concentration was interpreted as potential difference and the reading was displayed on the pH meter in millivolts. Thus, higher mV values referred to higher concentrations of dissolved carbon dioxide in the liquid. Once data in mV was collected, it was converted to concentration (ppm as CO_2) using the equation obtained from the calibration curve of the probe. (Omega Engineering Inc., 1992)

It was necessary to check the slope and calibrate the electrode every time before measuring the concentration of dissolved carbon dioxide in a solution. This ensured the correct operation of the electrode, and thus accurate results. The slope value was not supposed to be below 30 mV and above 62 mV. The higher slope value indicated higher resolution of the electrode, indicating higher accuracy of the electrode. If the slope was below or above the slope range as specified above, the electrode needed to be disassembled and left for 2 hours in the refill solution before using it (the electrode can be disconnected from the pH meter). Also, it was important to check if the electrode's membrane was not damaged as a slight scratch on it could interfere with the probe's performance.

3.3.2 Checking the Carbon Dioxide Electrode's Slope:

The slope of the carbon dioxide probe was checked on daily basis. In order to check the slope of the electrode, 5 ml of the buffer solution in the increments of 1 ml was added to the 45 ml of distilled water in a 100 ml beaker. The solution was stirred and 0.5 ml of standard carbon dioxide solution (1000 ppm as CO_2) was added. As soon as the probe was immersed inside the solution the negative mV values begin to decrease in magnitude. Once the mV value stabilized, it was zeroed by clicking on the "Rel mV" tab on the screen. Afterwards, 5 ml of the standard carbon dioxide solution was added in the increments of 1 ml, as soon as it was added the positive mV values began to increase in magnitude. The stabilized positive mV value determined the slope of the probe.

3.3.3 Generating the Calibration Chart of the Carbon Dioxide Electrode:

A calibration chart for the carbon dioxide probe was generated every time the electrode was re-assembled. The curve was generated using three standardized carbon dioxide solutions that is, 10, 100 and 1000 ppm as CO_2.The calibration was always performed from a 100 ppm as CO_2 solution therefore, 5 ml of the 1000 ppm as CO_2 solution was poured in the increments of 1 ml into the beaker containing distilled water and 5 ml of the buffer solution. The stable value noticed was zeroed in the same way as mentioned in Section 3.3.2. Then, the probe was immersed into 50 ml of 1000 ppm as CO_2 solution mixed with 5 ml of the buffer solution, a positive stable value was noted down after sometime. Then, the probe was immersed into the distilled water for 15 to 20 mintues before putting the probe into 10 ppm as CO_2 solution. This was done to bring the mV value to a big negative number because if the probe was immersed directly to the 10 ppm as CO_2 the mV values would have started to go down drastically without reaching a stable value. Thus, after leaving the probe inside distilled water, the probe was immersed into 10 ppm as CO_2 solution, which was a mixture of 49.5 ml of water, 0.5 ml of the standard carbon dioxide solution and 5 ml of the buffer solution. An increase in the magnitude of negative mV values was observed and eventually a stable value was obtained.

After having three mV values corresponding to the three standardized CO_2 solutions a logarithmic graph of potential difference (mV) vs. Concentration (ppm as CO_2) was generated by plotting the mV values against the corresponding concentrations of the CO_2 solutions in ppm as CO_2. The equation generated from the graph was used to convert the experimental data from millivolts to ppm as CO_2 to find the exact concentration of dissolved CO_2 in a solution.

It was required to calibrate the carbon dioxide probe before every run on daily basis. However, it was not mandatory to create the calibration chart everyday; immersing the probe into 10 ppm as CO_2 solution to set the mV value to zero was sufficient before doing the experiment. This step is called one-point calibration. But, if the probe was disassembled and was used again then it was necessary to generate a calibration curve.

More details about checking the slope and creating the calibration chart of the electrode are included in the ISE-8750 user manual.

3.3.4 Communication Interface between the Carbon Dioxide Probe and Computer:

An ion selective carbon dioxide electrode (Model no: ISE-8750, Omega, Laval, Quebec) was used to measure the concentration of dissolved carbon dioxide under various operating conditions in a carbon dioxide buffer solution inside a stirred tank bioreactor with the liquid volume of 10L (Bioflo 3000, Eppendorf New Brunswick, Mississauga, ON). In order to receive the probe's date on the computer, the probe was interfaced with the computer by following the steps as explained below.

The electrode was shipped dry; therefore, it was assembled first by following the instruction in the ISE-8750 user's manual, before the probe was interfaced with the computer. Once, the ion selective carbon dioxide electrode was assembled, it was connected to the pH meter (Accumet XL-50, Fisher Scientific, Ottawa,ON), and an interface between the pH meter and computer was developed using the software Accumet XLComm (Fisher Scientific, Ottawa, ON), which was ordered to setup the interface. In this way, all the readings from the ion selective electrode were displayed and stored on the computer.

The software XLComm was installed on the computer by following the instructions as specified in user's manual of XLComm. After the installation of the software the pH meter was connected

to the computer through RS-232 cable that came with the pH meter. Once the cable was connected, “COM Port Configuration” was performed by clicking on “Settings” and then “COM port configuration”. The dialog box as shown on page 16 of the XLComm’s manual appears on the screen. In the manual, it was specified to select “COM 1” but “COM 7” was selected as the COM Port because it was the only port that worked for the computer that was used. Otherwise, the exact steps as specified in the XLComm’s manual were followed thoroughly. (Fisher Scientific Company, 2007).

3.3.5 Communication Interface between the Bioreactor and Computer

Similarly, the software Track & Trend Biocommand (Eppendorf New Brunswick Scientific, Mississauga, ON) was ordered and installed on the PC by following the instructions in the user’s manual on page 17 to create an interface between the bioreactor and the PC (New Brunswick Scientific Company, 2009). The instructions as mentioned in the manual were followed throughout the time to setup the interface between the bioreactor and computer. However, in the case of configuration of NBS OPC Server, there were few instructions on page 32 of the user’s manual that were followed differently based on the personal experience.. For example, on the “Controller Search Wizard” window COM 6 was selected instead of COM 1 as mentioned in the manual. Further, BioFloProAB was chosen over Modbus or AFS Controllers as the bioreactor used in the experiment did not support Modbus or AFS Controllers. Otherwise, the instructions as specified in the manual were followed thoroughly to connect the bioreactor with the computer. The instructions about connecting the cables to the bioreactor and computer as mentioned in the user’s manual of the bioreactor Bioflo 3000 (Page 32-38) and the Track & Trend Biocommand software (Page 29-30) were exactly followed.

3.3.6 Design of the Carbon Dioxide Electrode Holder:

An electrode holder was designed for to hold the carbon dioxide electrode when inserted inside the bioreactor. It was used to ensure stability of the probe inside the bioreactor under turbulent conditions. It was made out of stainless-steel for durability and given a tilt of 25^{o} to prevent the formation of bubbles at the tip of the electrode. The angle of 25^{o} was chosen in this case based on the geometry of the insertion whole of the bioreactor. Otherwise, a tilt of 23^{o} would have been ideal to minimize the bubble formation at the tip of the electrode (Omega Engineering Inc.,

1992) . The detailed drawings of the hollow tube with the dimensions in millimetres are shown in Figure 3.1.

3.3.6.1 Insertion of the Carbon Dioxide Electrode inside the Holder

The carbon dioxide probe was inserted into the holder by positioning the holder such that its tilted portion faced the bottom. The cable of the probe was inserted first from the bottom end (tilted) until it could be pulled from the top end of the holder. The probe was pushed inside the holder from the bottom end of the holder until it tightly attached to it. Then, the screws were attached to strengthen the grip at the point where the top of the probe and bottom end of the pipe were tightly attached.

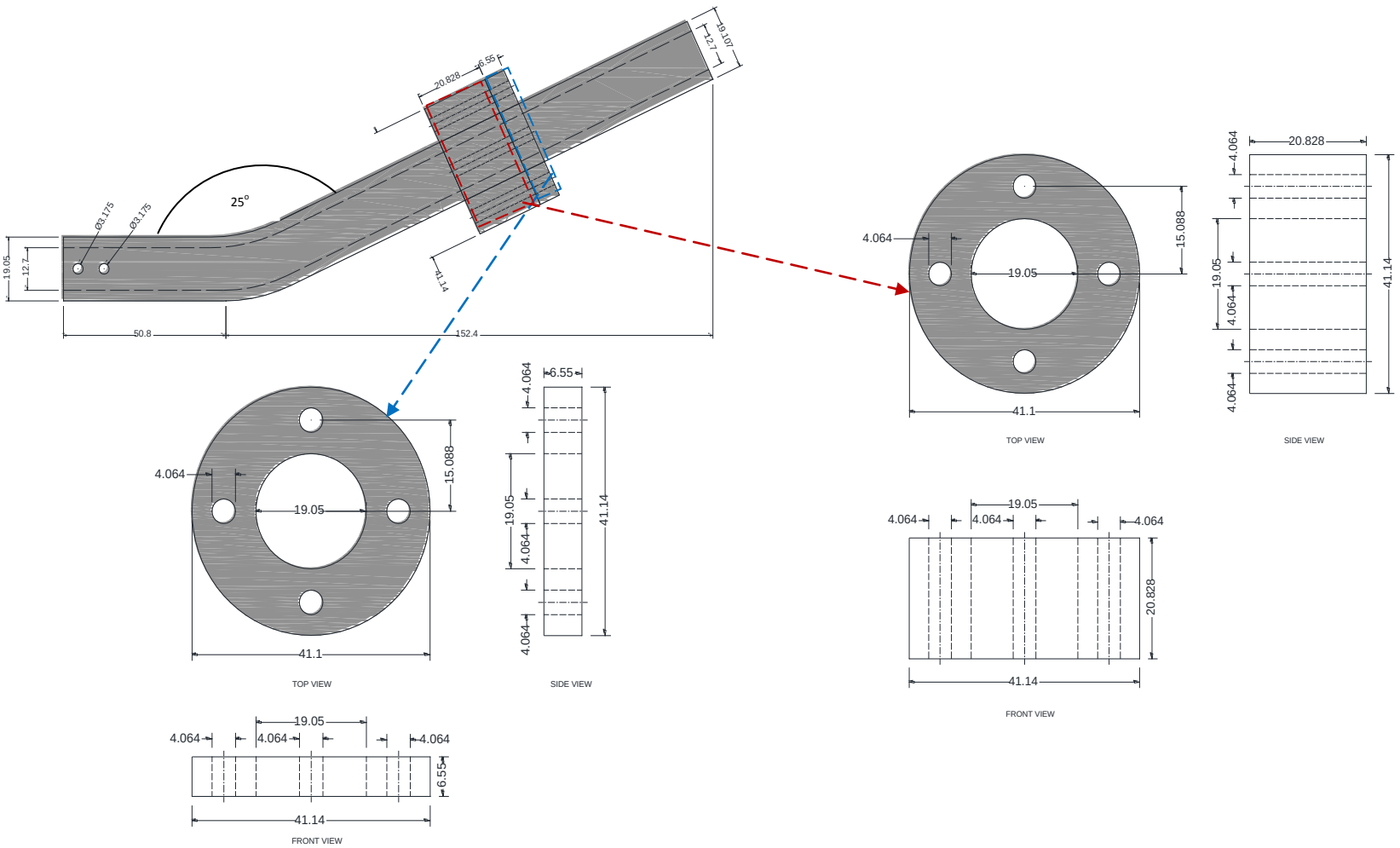

Figure 3.1: Detailed Sketch of the Stainless Hollow Tube

3.3.3 Experimental Setup:

A schematic diagram of the experimental setup is shown in Figure 3.2. It can be seen in the figure that CO_2 probe was inserted inside the bioreactor, and the mixture of 3% CO_2 mixed in air (v/v) was bubbled to the bioreactor from the rotameters. There were two rotameters that were used to mix CO_2 in air: CO_2 flowmeter tube (042-15-N,Omega, Laval, Quebec) with ±2% full-scale accuracy and 5 LPM air rotameter (Cole Parmer, Montreal, Quebec) with ±3% full-scale accuracy. The CO_2 flowmeter was connected to the carbon dioxide gas cylinder and the air rotameter was connected to the air valve. The rotameters were used to adjust and maintain the mixture of 3% CO_2 in air (v/v). The outlets of both rotameters were connected to a T-shaped valve to mix the two gases before they were bubbled to the bioreactor. Vinyl tubing with the inner and outer diameters of 0.008 m and 0.011 m respectively was used for the gas flow from one device to another. As shown in Figure 3.2, the gas bubbles when entered the bioreactor got smaller in size due to stirring. Also, a nitrogen cylinder was placed beside the bioreactor and was connected to the bioreactor in the case of pushing CO_2 out of the system to recycle the buffer solution for more experimental runs.

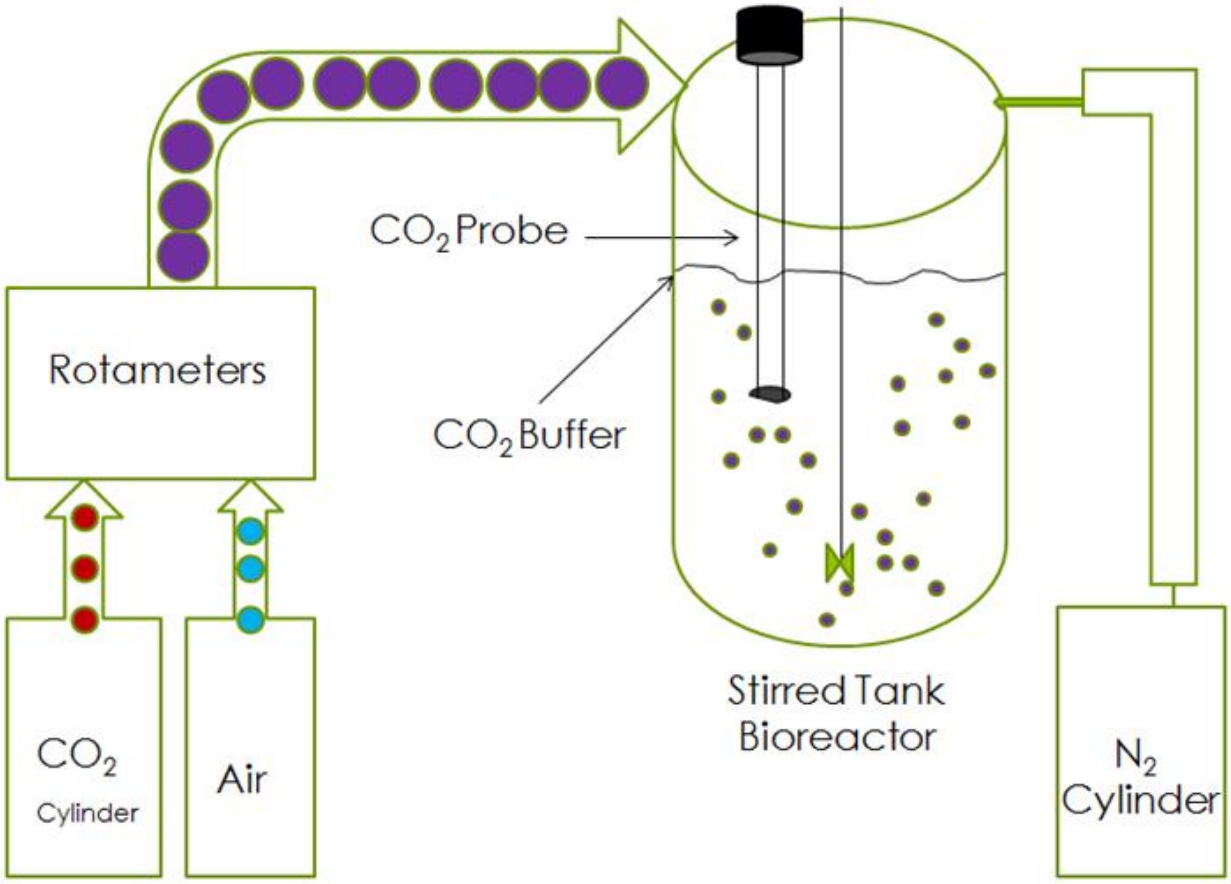

Figure 3.2: Schematic Diagram of the Experimental Setup

3.5 Experimental Procedure:

3.5.1 Filling Carbon Dioxide Buffer Solution in the Stirred Tank Bioreactor:

Inside the 14L stirred tank bioreactor, 10L of the buffer solution was prepared by first filling up the bioreactor with 2.5L of distilled water. The water was filled inside the bioreactor by connecting one end of the polyvinyl tubing to the distilled water tap and the other end was put inside the tank through the top opening. Then, 2940 grams of sodium citrate dihydrate was poured into the liquid by putting a funnel on the top of the bioreactor's opening; the stirring of the bioreactor was set at 400 rpm while pouring the chemical. The pH of the solution was brought to 4.5 by putting the concentrated hydrochloric acid diluted with water into the bioreactor in increments of 1L. During this process, the pH readings were measured by the pH probe of the bioreactor.

3.5.2 Measuring Dissolution of CO_2 inside the Stirred Tank Bioreactor:

After the bioreactor was filled with 10L of the buffer solution, 3% carbon dioxide in air (v/v) was bubbled to the 14L stirred vessel of the bioreactor. Throughout the time the bioreactor was set at the Fermentation mode. The readings were taken at the agitation rates of 150, 200, 300 and 400 rpm, and gas flowrates of 1100, 2000, 2900 and 3500 ml/min. The pH and temperature of the system were maintained at 4.5 and 25^{o}C respectively in all the runs. The pH was kept at 4.5 to minimize the interferences of carbonates and bicarbonates while measuring dissolved carbon dioxide in the sample. The temperature of 25^{o}C was maintained to keep the bioreactor operating at standard ambient temperature and pressure.

In each run, 3% of carbon dioxide mixed in air (v/v) was run until the saturation point of dissolved carbon dioxide was reached. All the readings overtime of dissolved carbon dioxide were recorded on the computer through the software XL-Comm. The mV values by the CO_2 probe were converted into concentration (ppm) values as explained earlier and the overall mass transfer coefficient (K_La) of CO_2 was measured from the plots as discussed in chapter 4.

3.6 Cleaning the Stirred Tank Bioreactor (Bioflo 3000):

Separating the vessel from the bioreactor system to autoclave it and replace the buffer solution is a very time consuming process. Therefore, a method to clean up the vessel without separating it from the machine was employed. In this method, the unwanted buffer solution was flushed out of the vessel using a peristaltic pump (913 Mity Flex). Subsequently, the vessel was filled up to 10L with distilled water through polyvinyl tubing and the agitation was turned on at 400 rpm for 1-2mins. Few minutes later, agitation was stopped and distilled water was flushed out in the same way as mentioned earlier. The same cycle of pouring and flushing of distilled water from the bioreactor was repeated 3 to 4 times to ensure the vessel is sufficiently clean for more experiments without any contamination.

Chapter 4: Results & Discussion

4.1 On-line Measurement of Dissolved Carbon Dioxide inside the Stirred Tank Bioreactor

The carbon dioxide probe was immersed inside the bioreactor and the concentration of dissolved carbon dioxide was recorded overtime. The readings were recorded initially as the potential difference induced by the change in the pH of the refill solution after the passage of the dissolved CO_2 through the membrane of the probe. Therefore, the readings obtained through on-line measurements of dissolved carbon dioxide were in millivolts.

The calibration curve in Figure 4.1 was created and used to convert the potential difference (mV) values into the concentration (ppm as CO_2) values. The calibration curve was developed using the standardized solutions of carbon dioxide to find out the corresponding concentration values of the mV values as displayed by the probe. The method to generate such a calibration curve for the carbon dioxide probe is explained in Section 3.6 of Chapter 3.

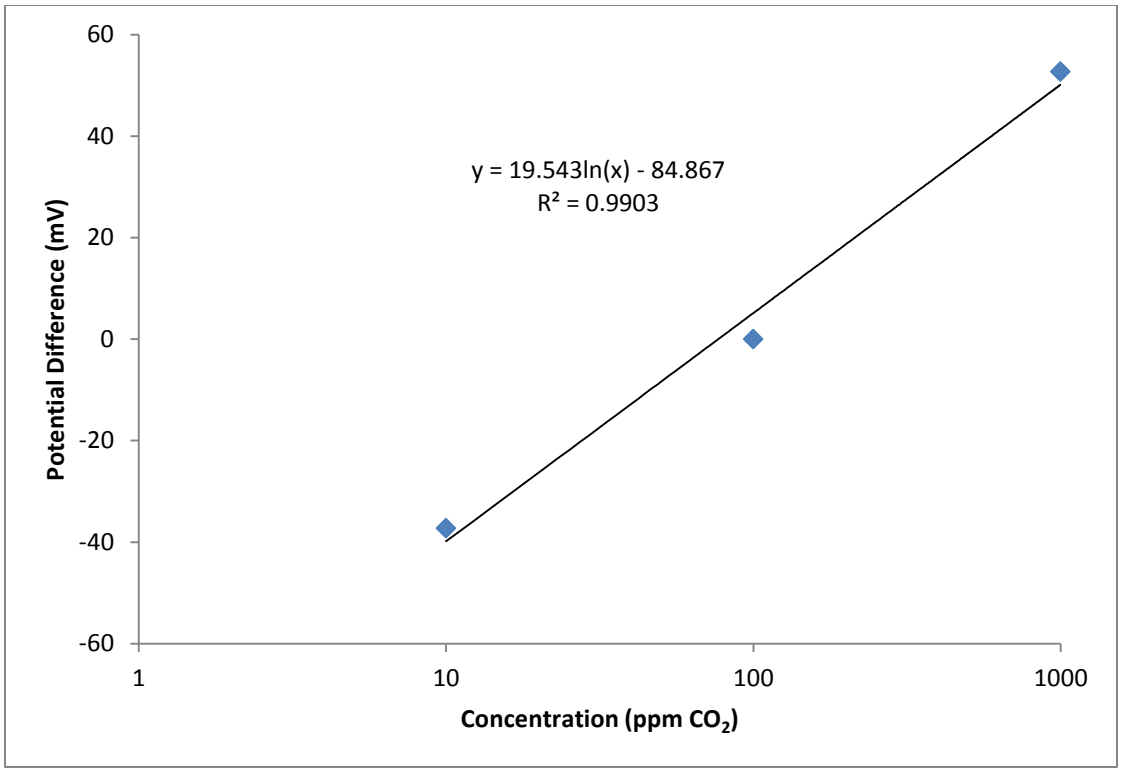

Figure 4.1: Calibration Curve for the Carbon Dioxide Electrode

Figure 4.2 below shows the curves generated while taking on-line measurements of dissolved carbon dioxide; at the time 3% CO_2 mixed in air was bubbled into the system at 2000 ml/min and various agitation rates. It can be seen in the figure that over time the curve became less steep and eventually flattened showing the saturation point of dissolved CO_2. The saturation point of CO_2 refered to the point at which solubility of CO_2 was at its maximum in the solvent.

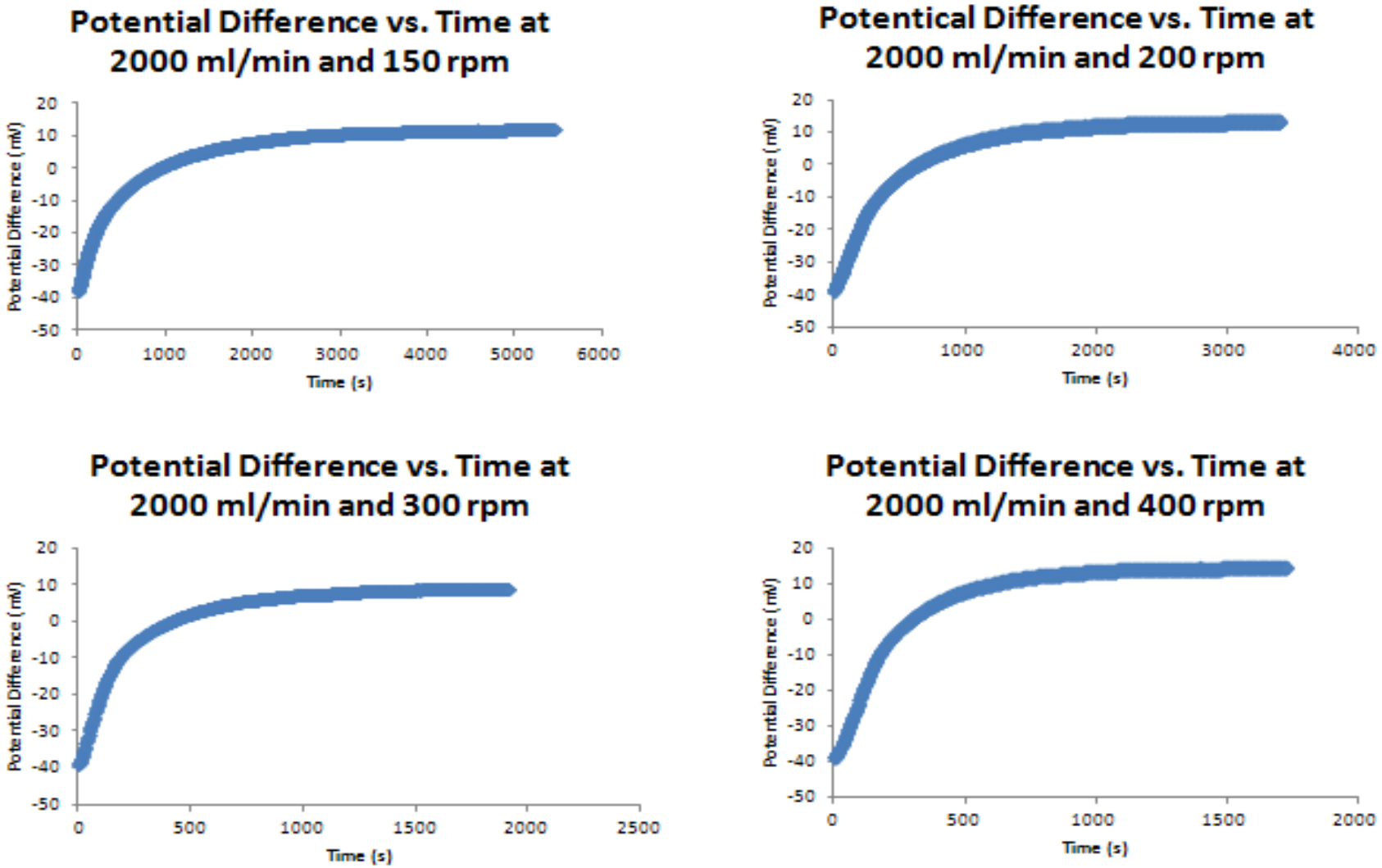

Figure 4.2: Change in mV values Over Time as Carbon Dioxide was Dissolved in the Buffer Solution inside the Stirred Tank Bioreactor

The potential difference data in millivolts from Figure 4.2 was converted to the concentration (ppm as CO_2) data, and was plotted against time as shown in figure 4.3. The data in millivolts was transformed into ppm as CO_2 using the equation obtained from the calibration chart of the carbon dioxide probe as illustrated in Figure 4.1. The method to generate the calibration chart for the carbon dioxide is explained in Section 3.4.2 of Chapter 3.

In Figure 4.3, similar shapes of the curves were achieved as in Figure 4.2 showing the concentration of saturated dissolved carbon dioxide as the graphs flattened. It was noticed from Figure 4.3 that as the agitation rate was increased while keeping the flowrate the same the saturation point was reached more quickly. Hence, it can be concluded that the agitation rate is directly proportional to the rate of dissolution of CO_2.

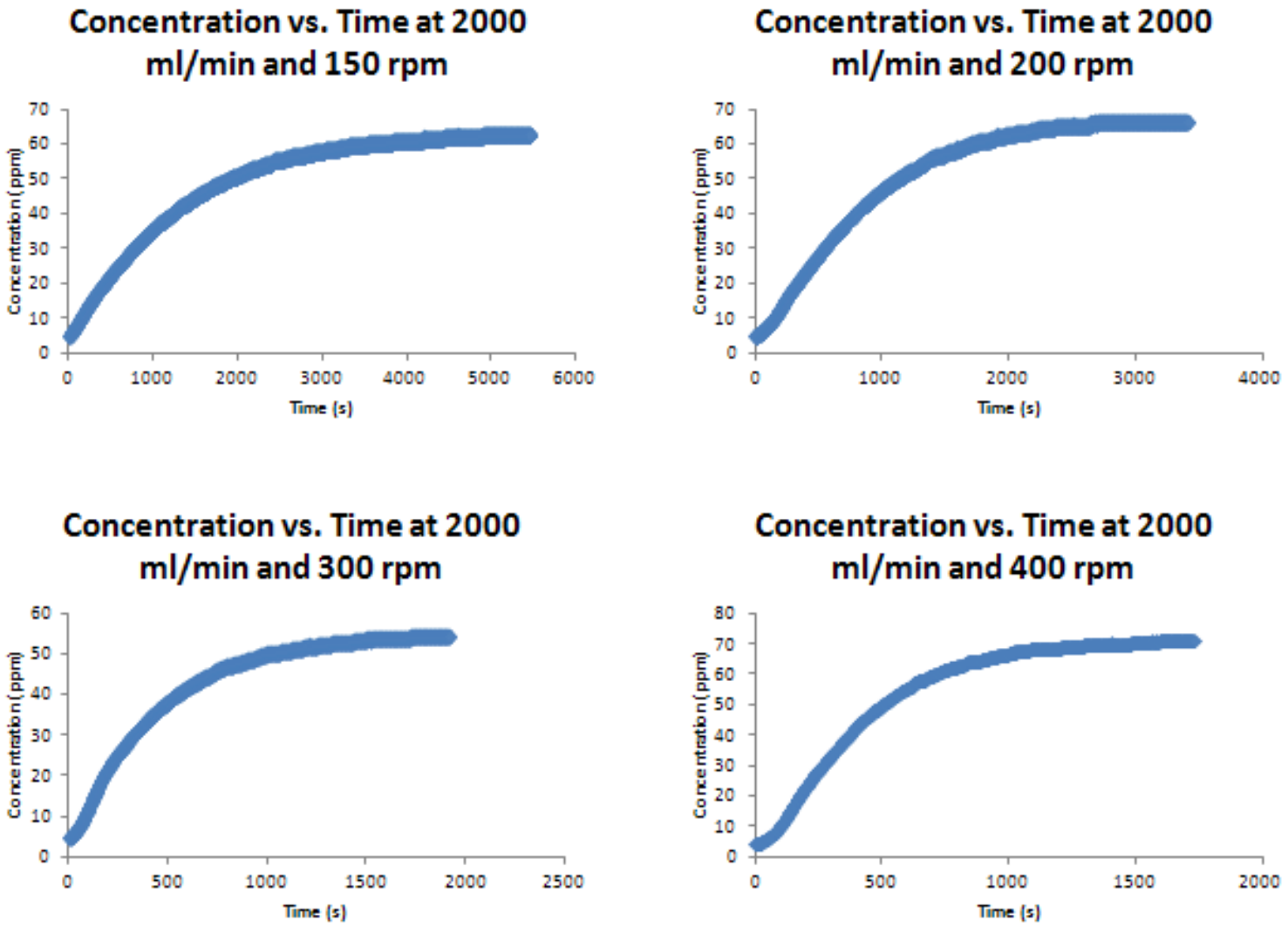

Figure 4.3: Change in the Concentration of Dissolved Carbon Dioxide over Time

4.2 Experimental Determination of $K_L a$ from CO_2 Data:

Overall volumetric mass transfer coefficient ($K_L a$) of carbon dioxide was determined for the data as illustrated in Figure 4.2 by following the calculations as explained below:

The equation of the mass transfer coefficient was considered to perform the experiment:

$$N_a = K_L a(C^* - C) \tag{4.1}$$

Since $N_a = \frac{dc}{dt}$ Equation 4.1 can be written as

$$\frac{dc}{dt} = K_L a(C^* - C) \tag{4.2}$$

Equation 4.2 was integrated on both sides as shown below:

$$\int_{C_o}^{C} \frac{dc}{(C^* - C)} = K_L a \int_{t_o}^{t} dt \tag{4.3}$$

Thus, Equation 4.4 was obtained

$$ln\,[(C^* - C)/(C^* - C_o)] = K_L a\,(t - t_o) \tag{4.4}$$

The graphs as shown in Figure 4.4 were generated by plotting Equation 4.4, and the slope of the curves gave $K_L a$ values in per second for each agitation rate at 2000 ml/min. In the experiment, C_o is the initial concentration of dissolved carbon dioxide at t_o and t_o was zero as it refers to the initial time of the experimental run.

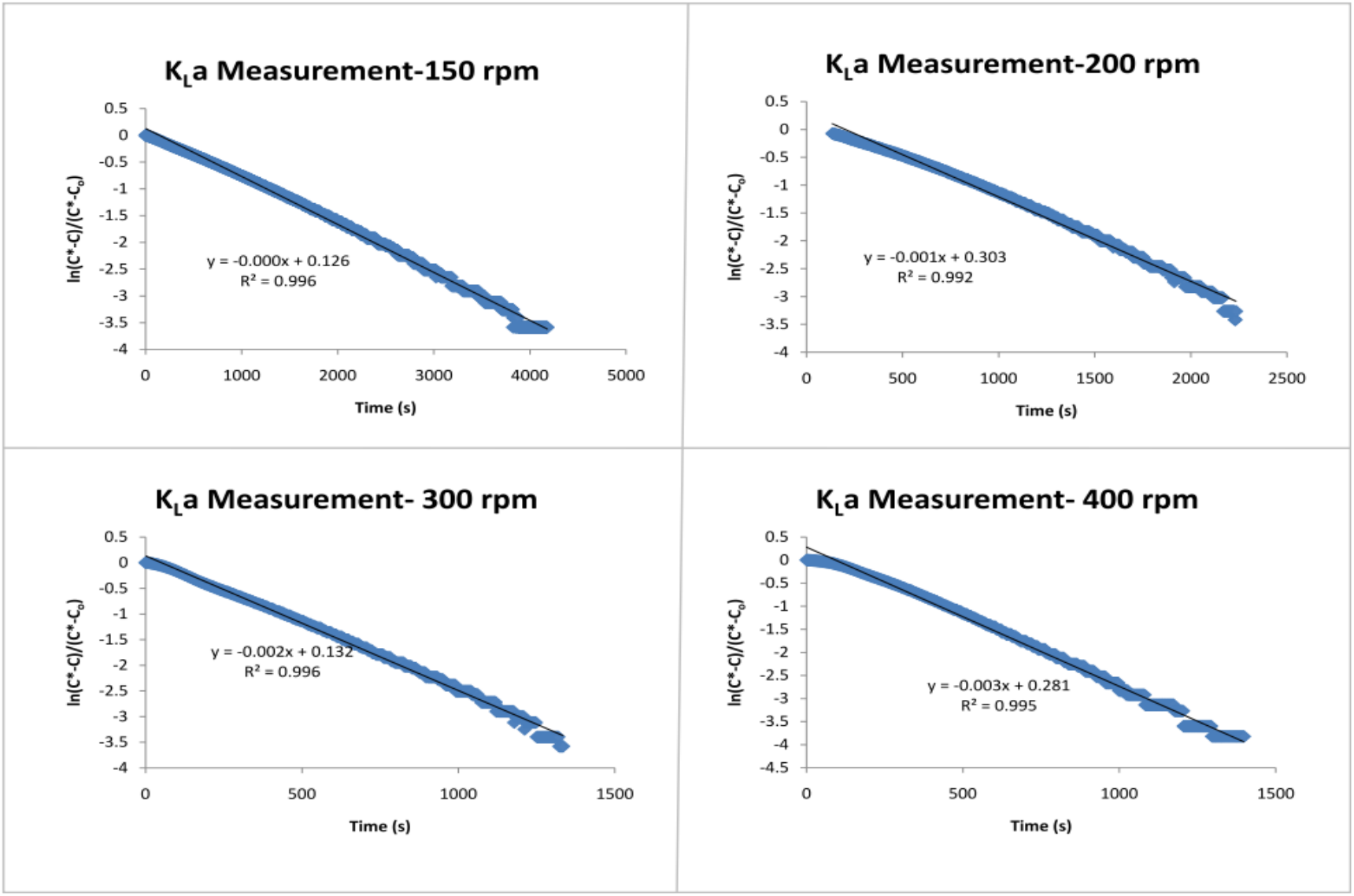

Figure 4.4: Measurement of Overall Volumetric Mass Transfer Coefficient of Carbon Dioxide at 2000 ml/min and various Agitation Rates

Absolute values of the slope were considered from the Figure 4.4. For example: 0.0009, 0.0015, 0.0026 and 0.003/s because the negative sign only refers to the direction of mass transfer from concentration to low concentration. The units of K_La values obtained from Figure 4.4 were converted from per second to per hour to analyze the impact of each operating parameter on K_La. Please refer to appendices for K_La curves for other conditions.

4.3 Effect of Agitation Rate and Flowrate on the Overall Volumetric Mass Transfer Coefficient (K_La) of Carbon Dioxide in a Stirred Tank Bioreactor

The effect of agitation rate and flowrate on K_La of carbon dioxide was analyzed. The K_La values obtained for each case scenario are tabulated in Table 4.1 as shown below:

Table 4.1: Overall Volumetric Mass Transfer Coefficients of Carbon Dioxide at Different Agitation Rates and Flowrates

	K_La (/h)			
Flowrate (ml/min)	**1100**	**2000**	**2900**	**3500**
Agitation Rate (rpm)				
150	3	3.36	3.72	4.32
200	4.44	4.92	6.12	6.6
300	7.2	9.48	9.48	9.48
400	10.8	14.16	13.68	12.72

The K_La values of carbon dioxide as shown in Table 4.1 were compared to the values as reported by Kordac and Linek (2008). The experimental data obtained showed the similar pattern that is, increase in K_La values with the increase in agitation rate. However, the values reported by Kordac and Linek (2008) were higher than the values obtained in this experiment because their bioreactor was under different operating conditions than the conditions used in this study. Also, the results obtained in the table were in coherence with the results reported by Hill (2006). He reported a direct relationship of K_La with gas flowrate and this was observed in this experimental work as well.

However, an exception was noticed at 300 rpm when the flowrate was higher than 2000ml/min there was no change in the overall mass transfer coefficients of carbon dioxide. Hence, there was no impact of flowrate on K_La of carbon dioxide at 300 rpm above the flowrate of 2000 ml/min. This observation could be due to higher gas hold ups which act as threshold and prevent the increase in K_La as the flowrate is increased at 300 rpm. However, once this threshold was crossed as the agitation rate was increased from 300 rpm to 400 rpm, the overall mass transfer coefficients began to decrease in value as the flowrate became higher than 2000 ml/min.

Usually as the gas hold up increases K_La increases, but, it is possible to have an inverse relationship between the gas hold up and K_La showing a reduction in K_La with an increase in the gas hold up. An inverse relationship was reported between the gas hold up and K_La in a tubular system as the superficial gas velocity became higher than 0.075 m/s (TK Ghosh et al., 2010). This shows that there is a certain gas flowrate beyond which the direct relationship between the gas hold up and K_La changes to an inverse relationship. In this experiment, the gas flowrate of 2000 ml/min and agitation rate of 300 rpm was the threshold point. Before this threshold point the K_La increased as the gas hold up increased showing coherence with the results as reported by Singh and Majumdar (2010).

However, at a specific flowrate, increase in agitation rate caused an increase in K_La as well as gas hold up. This phenomenon is illustrated in Figures 4.5 and 4.6 below:

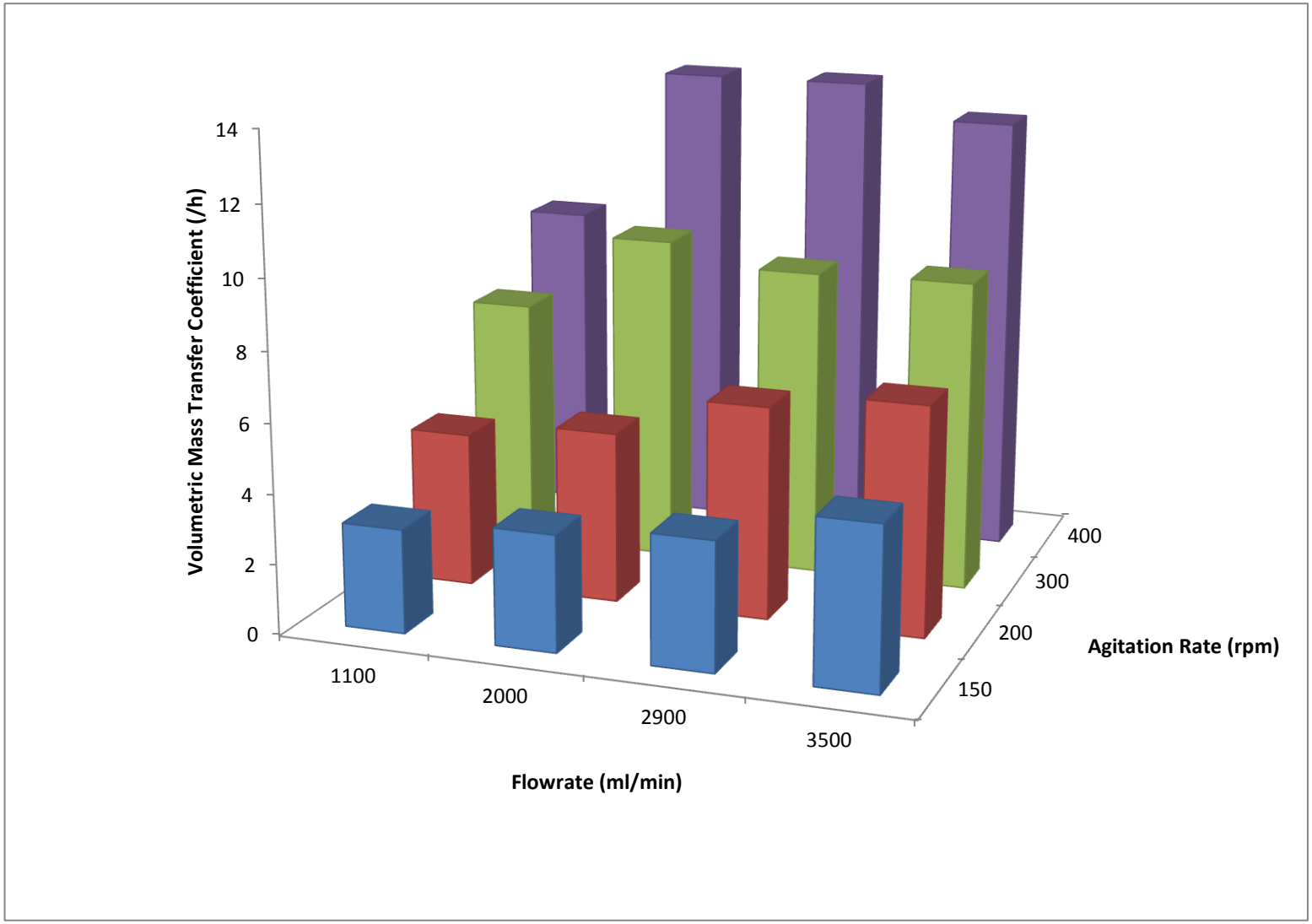

Figure 4.5: Overall Volumetric Mass Transfer Coefficient of Carbon Dioxide as a Function of Flowrate and Agitation Rate

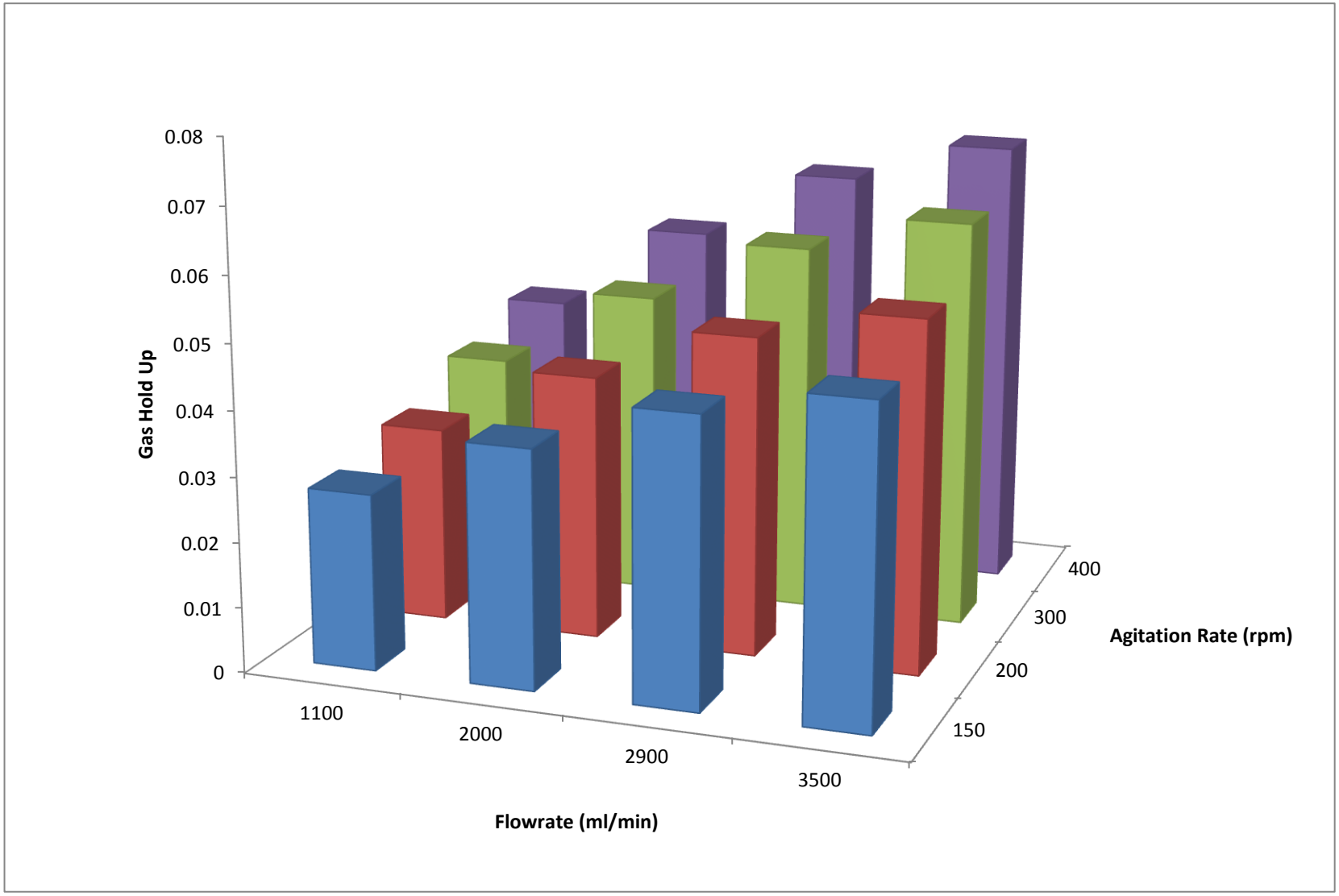

Figure 4.6: Gas Hold Up as a Function of Gas Flowrate and Agitation Rate

It is important to note that unlike the dependence of K_La on agitation rate and flowrate, there is no threshold for the gas hold up values. In other words, the gas hold up was found to be directly proportional to the agitation rate and flowrate all the time.

Gas hold ups as plotted in Figure 4.6 were calculated by using the following correlation:

$$h = 1.8 \left(\frac{P}{V}\right)^{0.14} (U_g)^{0.75} \quad (4.5)$$

(Lydersen et al., 1994)

where, P is aerated power in Watts, V is the volume of aerated liquid in m^3 and Ug is superficial velocity, which is the ratio of the volumetric gas flowrate (m^3/s) to the cross-section area of the bioreactor (0.14 m^2). In this work, gas hold ups were calculated using P as calculated in Equation 4.12.

Figure 4.7 below demonstrates the change in the overall volumetric mass transfer coefficient of carbon dioxide and gas hold up as the agitation rates are changed at certain flowrates. The graphs show a direct relationship of the overall mass transfer coefficient and gas hold up. The error bars in Figure 4.7 refer to the values with 95% confidence interval.

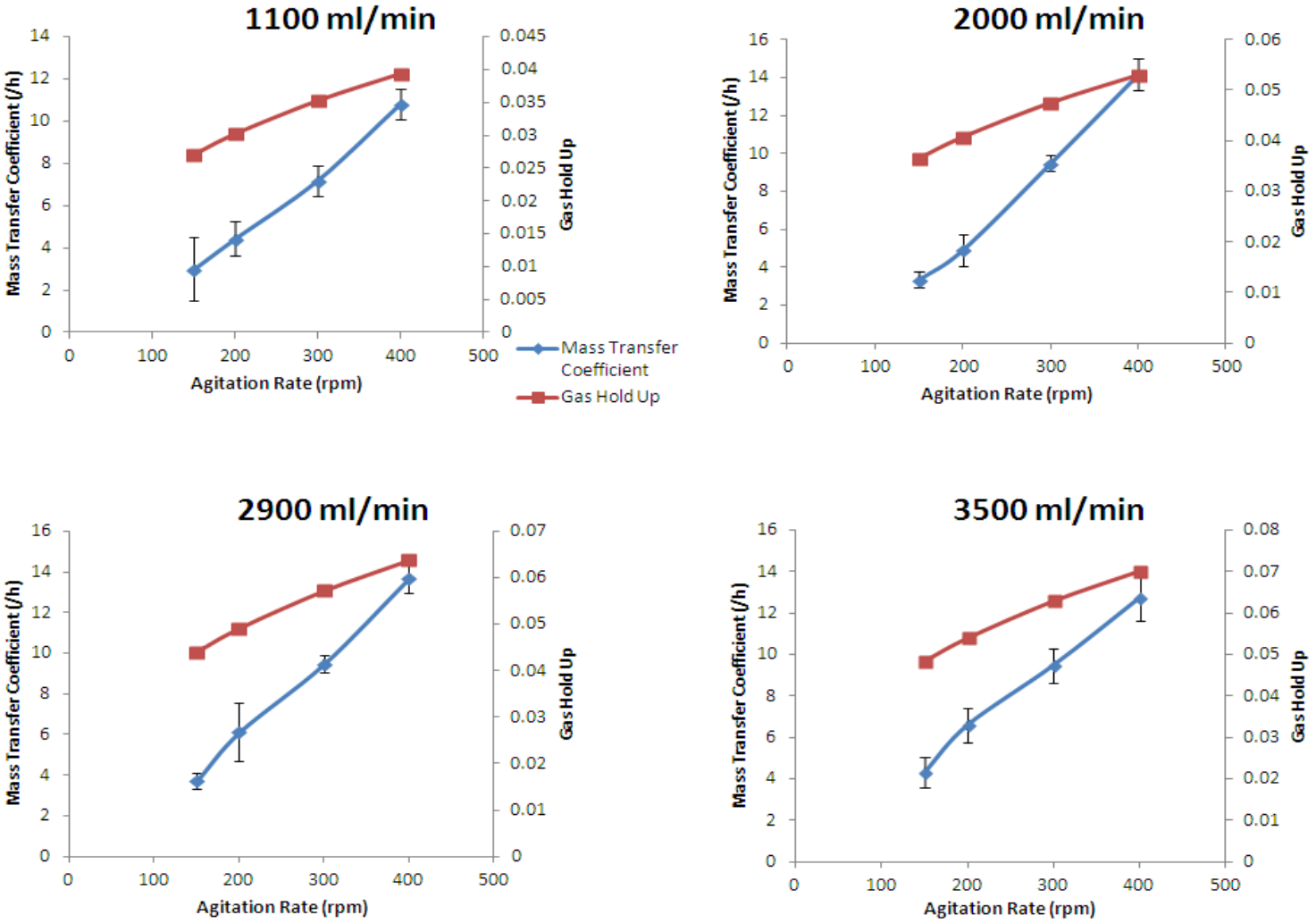

Figure 4.7: Impact of Flowrate and Agitation Rate on the Rate of Increase of Volumetric Mass Transfer Coefficient and Gas Hold Up

It can be seen in the figure above that the rate of increase in gas hold up is not affected by the increase in flowrate and agitation rate. Whereas, the rate of increase in overall volumetric mass transfer coefficient above the flowrate of 2000 ml/min slows down a bit as the agitation rate goes up. In fact, the curves for K_La in the above figure become less steep at the flowrates above 2000 ml/min. In addition to the increased gas hold up there was high turbulence inside the system as the gas flowrate and agitation rates were increased.

For example, Figure 4.8 illustrates the change in turbulence inside the stirred tank bioreactor at the time the gas flowrate was kept at 2000 ml/min and different agitation rates. At higher agitation rates higher turbulence was observed with decreased bubble size and increased number of bubbles in the system. For example, at lower agitation rates such as 150 and 200 rpms there were less bubbles but their size was bigger. Whereas, at 300 and 400 rpms there was more turbulence in the system and there were many bubbles that are smaller in size. In the same way, at the flowrates beyond 2000 ml/min, there was more turbulence in the bioreactor than shown in the figure below. Thus it can be concluded that at higher gas flowrates and agitation rates, the gas hold up and turbulence become very high. As a result, microbubbles (very small bubbles) are formed showing high interfacial area but do not participate in the mass transfer process, causing K_La to increase at a lower rate than expected (Cents, 2003). For this reason, in the experiment, above the flowrate of 2000 ml/min the rate of K_La increase slowed down due to high turbulence and gas hold up inside the system.

2000 ml/min

150 rpm

200 rpm

300 rpm

400 rpm

Figure 4.8: Turbulence inside the Bioreactor at various Agitation Rates

4.4 Investigating Parameters for Enhanced Overall Volumetric Mass Transfer Coefficient of CO_2

Once all data was collected it was plotted to find the combination of flowrate and agitation rate for enhanced K_La of CO_2. This investigation was important to minimize power and CO_2 consumption, yet obtaining high value for K_La of CO_2.

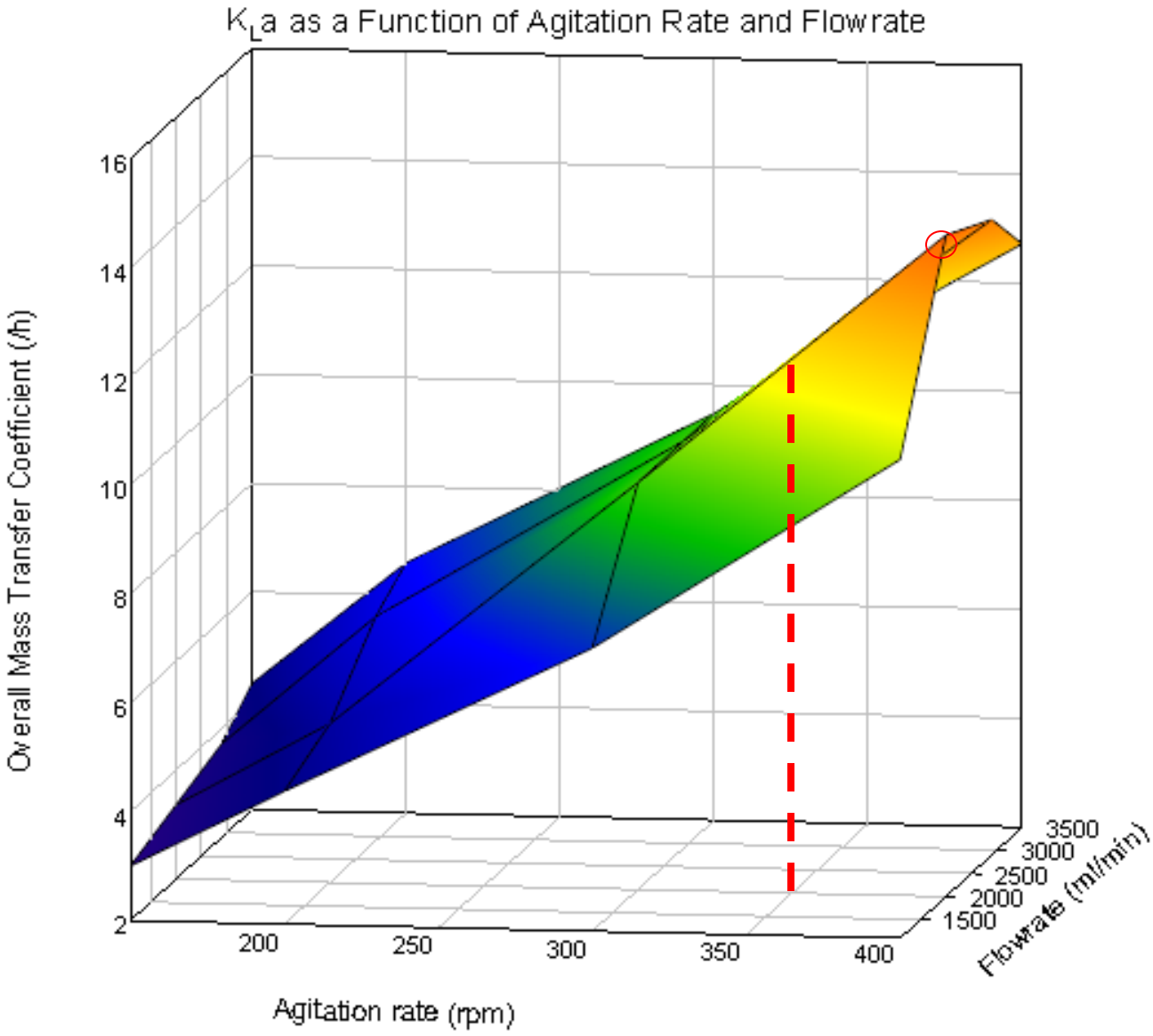

Figure 4.9: Determination of the Combination of the Agitation Rate and Gas Flowrate for Enhanced Overall Volumetric Mass Transfer Coefficient of Carbon Dioxide

From a 3D plot in Figure 4.9 it is found that a peak, which is circled in red at the flowrate of 2000 ml/min gives highest volumetric mass transfer coefficient. The agitation rate at the circled peak is 400 rpm, but this agitation rate requires higher power consumption. Therefore, if the agitation rate is reduced from 400 rpm to 350 rpm, there will be decrease in the power consumption from 2.8 to 1.8 Watts; hence there is a saving of 1 Watt. Furthermore, the K_La value will still be close to the orange region as it is for 400 rpm as shown by red dashed line in Figure 4.9, showing a high value of overall volumetric mass transfer coefficient of CO_2. Thus, 2000 ml/min and 350 rpm were considered as the optimum conditions for enhanced mass transfer of CO_2 into liquid and microalgae cultivation inside the bioreactor.

4.5 Theoretical Development of Correlations of K_La for Carbon Dioxide inside a Stirred Tank Bioreactor

Generally, correlations that are used to calculate the overall mass transfer coefficient of a dissolved gas in a stirred tank vessel have the form as shown below:

$$K_L\,a = a\left(\frac{P}{V}\right)^{b}\left(U_{gs}\right)^{c} \tag{4.6}$$

where, a, b and c are constant values which depend on the type of gas being used and operating conditions of the stirred tank reactor. P is the power exerted by the stirrer to the aerated liquid in Watts (W), V is the volume of liquid inside the tank in m^3 and U_{gs} is superficial gas velocity in m/s. (Doran, 1995)

Until now, several values of a, b and c are reported to determine the volumetric mass transfer coefficient of oxygen in an agitated vessel under various operating conditions. On the other hand, for carbon dioxide there is not enough information available about the constant values to calculate K_La of CO_2.

Therefore, based on the experimental results obtained constant values of a,b and c were generated using Microsoft Excel, and correlations were developed to directly calculate the overall volumetric mass transfer coefficient of carbon dioxide. Two methods were employed to determine power (P) and superficial gas velocity (U_{gs}), hence K_La correlations were developed corresponding to each method.

4.5.1 Calculating Individual Parameters of Equation 4.4

The superficial gas velocity U_{gs} was determined by multiplying superficial velocity with gas hold up (as calculated using Equation 4.5).

Power (P) in the Equation 4.6 was determined by first calculating power for non-aerated liquid using the following correlation:

$$\frac{P}{V} = 6\,x\,10^{-12}\,Re^{2.921}, Re > 10^4 \quad (4.7)$$

(Taghavi et al., 2011)

where, V = 0.01 m^3

Once, the power for non-aerated liquid (P) was determined, power for aerated liquid (P_g) was calculated using the correlation for dual Rushton impeller stirred tanks, which is as follows:

$$\frac{P_g}{P} = 0.19(Flg)^{-0.28}(Fr)^{0.127}\left(\frac{W}{D}\right)^{0.18}\left(\frac{D}{D_t}\right)^{-0.65} \quad (4.8)$$

(Taghavi et al., 2011)

where, D_t is the diameter of the bioreactor, which was 0.21 m, D is the impeller diameter which was 0.08m for the six-bladed Rushton turbine used in the experiment, W is the width of the impeller, which was 0.022 m.

On the other hand, Fr in Equation 4.8 is Froude's Number which was determined using Equation 4.8.

$$Fr = \frac{N^2 D}{g} \quad (4.9)$$

(Taghavi et al., 2011)

Where, N is agitation rate of the impeller inside the bioreactor in revolutions per second (rps) and g is the acceleration due to gravity, which is 9.8 m/s^2.

Flg is the Gas Flow Number, which is dependent on Froude's number, and varies for the lower and upper impellers as both impellers experience flooding-loading transition. In the experimental runs, both impellers were assumed under flooding-loading transition; therefore, the following two equations were used to calculate Flg of each impeller:

Gas Flow Number for the Lower Impeller:

$$Flg_l = 0.25(Fr)^{0.75} \quad (4.10)$$

Gas Flow Number for the Upper Impeller:

$$Flg_u = 1.08(Fr) \quad (4.11)$$

(Taghavi et al., 2011)

There are two different equations to determine Flg of each impeller because the upper impeller completes the transition at lower speed than the lower impeller. (Taghavi et al., 2011)

Since Flg for each impeller was calculated separately, power exerted by each impeller was also determined separately. For example, Flg from Equation 4.10 was substituted in Equation 4.8 and the power P_{gl} was calculated for the lower impeller. Then, Flg from Equation 4.11 was substituted in Equation 4.8 to calculate the power P_{gu} for the upper impeller. Once, P_g for each impeller was determined, total power of the entire dual impeller was calculated by summing up P_{gl} and P_{gu}, and this total power was used in Equations 4.16and 4.17 to calculate K_La of CO_2.

$$P_{gTot} = P_{gl} + P_{gu} \quad (4.12)$$

The Gas Flow Number that should be used to determine the aerated power of both upper and lower impellers simultaneously is not specified. Therefore, the aerated power from the method as described above was plotted as "Equation 4.12" in Figure 4.11, and compared with the aerated power determined using various Flg values as calculated from different approaches. The figure below illustrates the results obtained after each method was employed, and it was found that the method as mentioned above gave the most appropriate results.

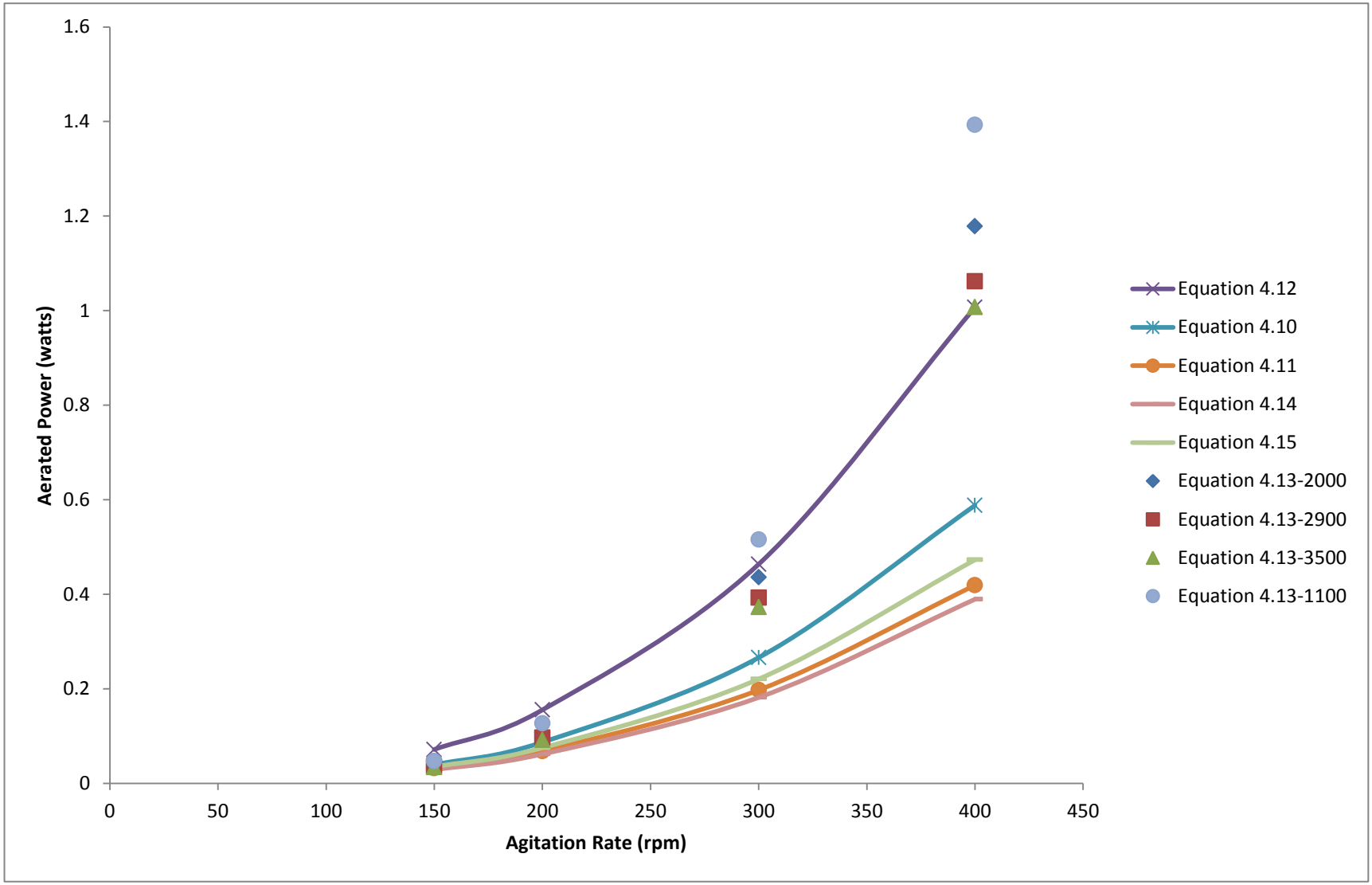

Figure 4.10: Comparison of Aerated Power Determined Using Various Methods

In Figure 4.10, the curves “Equation 4.13-1100”, “Equation 4.13-2000”, “Equation 4.13-2900” and “Equation 4.13-3500” refer to the aerated powers determined for the gas flowrates of 1100, 2000, 2900 and 3500 ml/min by using Flg calculated from the following equation, which is usually used for single impellers:

$$Flg = \frac{Q_g}{ND^3} \tag{4.13}$$

(Taghavi et al., 2011)

Where, Q_g is the gas flowrate (m^3/s), N is the agitation rate (revolutions per second), and D is the impeller diameter (m).

Whereas the curves “Equation 4.14” and “Equation 4.15” indicate the aerated power determined after summing up and averaging the Flg values respectively as shown in Equations 4.14 and 4.15. On the other hand, “Equation 4.10” and “Equation 4.11” curves were generated using Flg for lower and upper impellers respectively.

$$Flg_{sum} = Flg_l + Flg_u \tag{4.14}$$

$$Flg_{Avg} = \frac{Flg_l + Flg_u}{2} \tag{4.15}$$

From the curves as plotted in Figure 4.11, it was noticed that the curve “Equation 4.12” gave values of the aerated power that were either higher or close to the values in the curves “Equation 4.13-1100”, “Equation 4.13-2000”, “Equation 4.13-2900”, and “Equation 4.13-3500” which were created assuming single impeller. This observation was expected because it was anticipated to have higher power values exerted by two impellers than by a single impeller. In contrast, the curves “Equation 4.10”, “Equation 4.11”, “Equation 4.14” and “Equation 4.15” provided lower power values than the curves that were generated based on the assumption of a single impeller. For this reason, the approaches employed for the curves “Equation 4.10”, “Equation 4.11”, “Equation 4.14” and “Equation 4.15” were not considered because there were two impellers in operation instead of one, and it was expected to have a higher power from a dual impeller than a single impeller. Therefore, the approach employed for the curve “Pa Total” was considered to calculate the aerated power in the experiment.

4.5.2 K_La Correlations for Carbon Dioxide in a Stirred Tank Bioreactor:

The Correlations 4.16 and 4.17 below were developed to calculate K_La of CO_2 after P and U_{gs} were calculated using the equations that are explained later in the section.

The Correlation 4.17 below was developed for a stirred tank bioreactor having 3% CO_2 in air at the flowrate of 1100 ml/min and agitation rate in the range of 150-400 rpm.

$$K_L\, a = 1.148 \left(\frac{P}{V}\right)^{0.4846} \tag{4.16}$$

Whereas, for a stirred tank bioreactor with 3% CO_2 in air at the flowrate and agitation rate in the range of 2000-3500 ml/min and 150-400 rpm respectively the following correlation was created:

$$K_L\, a = 1.663 \left(\frac{P}{V}\right)^{0.464} \left(U_{gs}\right)^{0.0014} \tag{4.17}$$

It is important to note that Equation 4.16 does not have an U_{gs} term, because at a lower flowrate as in the case of 1100 ml/min, the power of U_{gs} became zero, showing a negligible impact on K_La. For this reason, it can be concluded that superficial gas velocity is negligible at a very low gas flowrate. This negligible effect of U_{gs} on K_La can be explained because of the lower gas hold up, which affects U_{gs}. Figure 4.11 below shows the degree to which the gas flowrate influences the gas hold up that is, there is a big gap between the of 1100 ml/min and 2000 ml/min. It can be seen in the figure how gas hold up increased significantly as the gas flowrate was raised above 1100 ml/min. Therefore, at 2000 ml/min and above the superficial gas velocity is more significant than below 2000 ml/min.

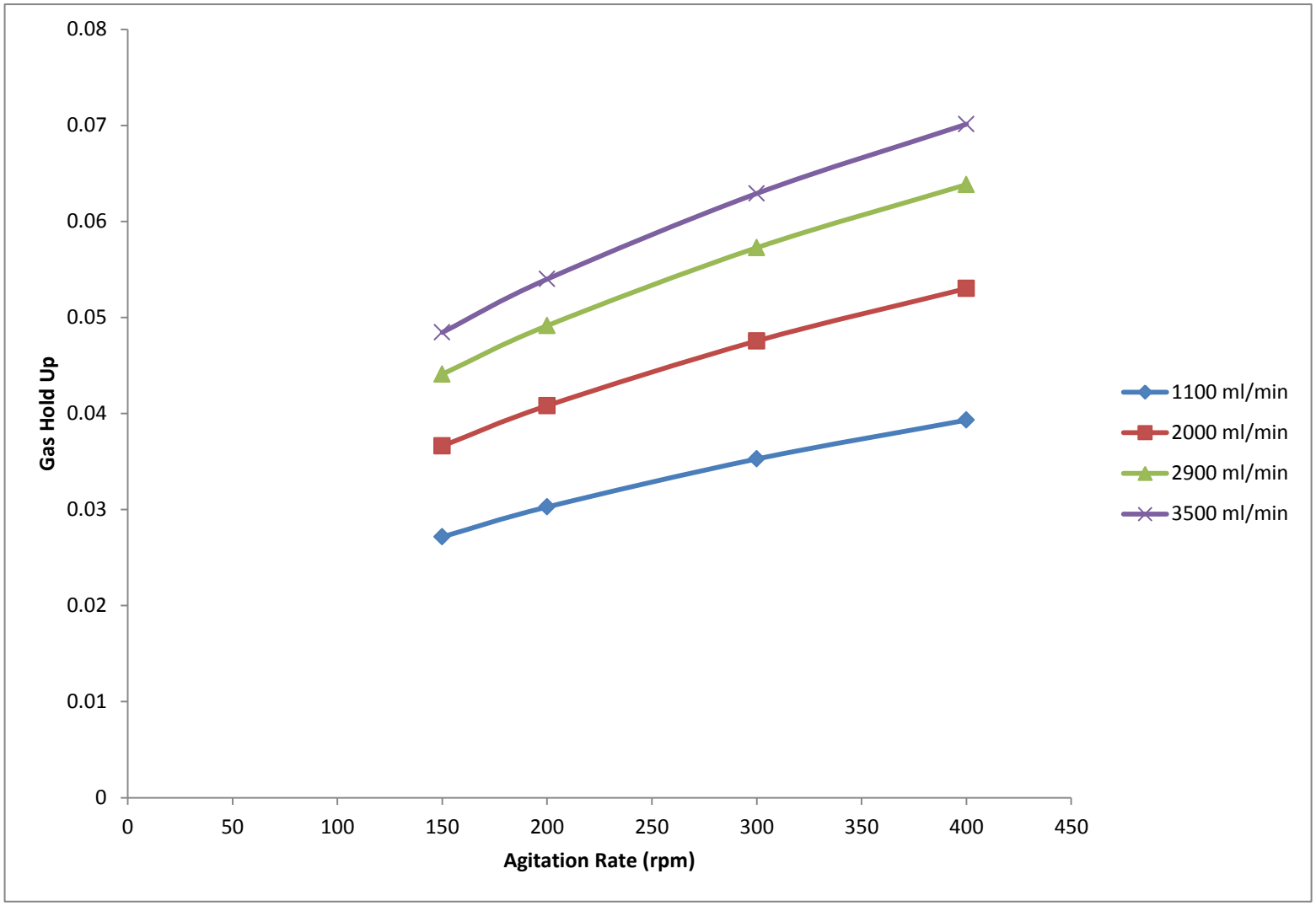

Figure 4.11: Gas Hold Up as a Function of Agitation rate and Flowrate

4.5 Validity of the Developed K_La Correlations:

The K_La values obtained through the correlations as mentioned in Section 4.4.2 were compared with the experimental K_La values to check the validity of the correlations. It was necessary to validate the correlations because for each gas flowrate a correlation was developed at the agitation rates ranging from 150-400 rpm. Once the a, b, c values were found for each correlation, they were averaged to develop a single correlation that was applicable to all the gas flowrates. However, two correlations were developed: one for the very low gas flowrate and the other for higher gas flowrates as it was not possible to fit the data of the lower gas flowrate into the correlation of higher gas flowrates. For this reason, the following graphs were created to analyze how well the experimental data fit with the calculated data from the correlation based on the average values of a, b, c for higher gas flowrates.

Figure 4.12 below shows a comparison between the experimental and calculated data from Equation 4.16.

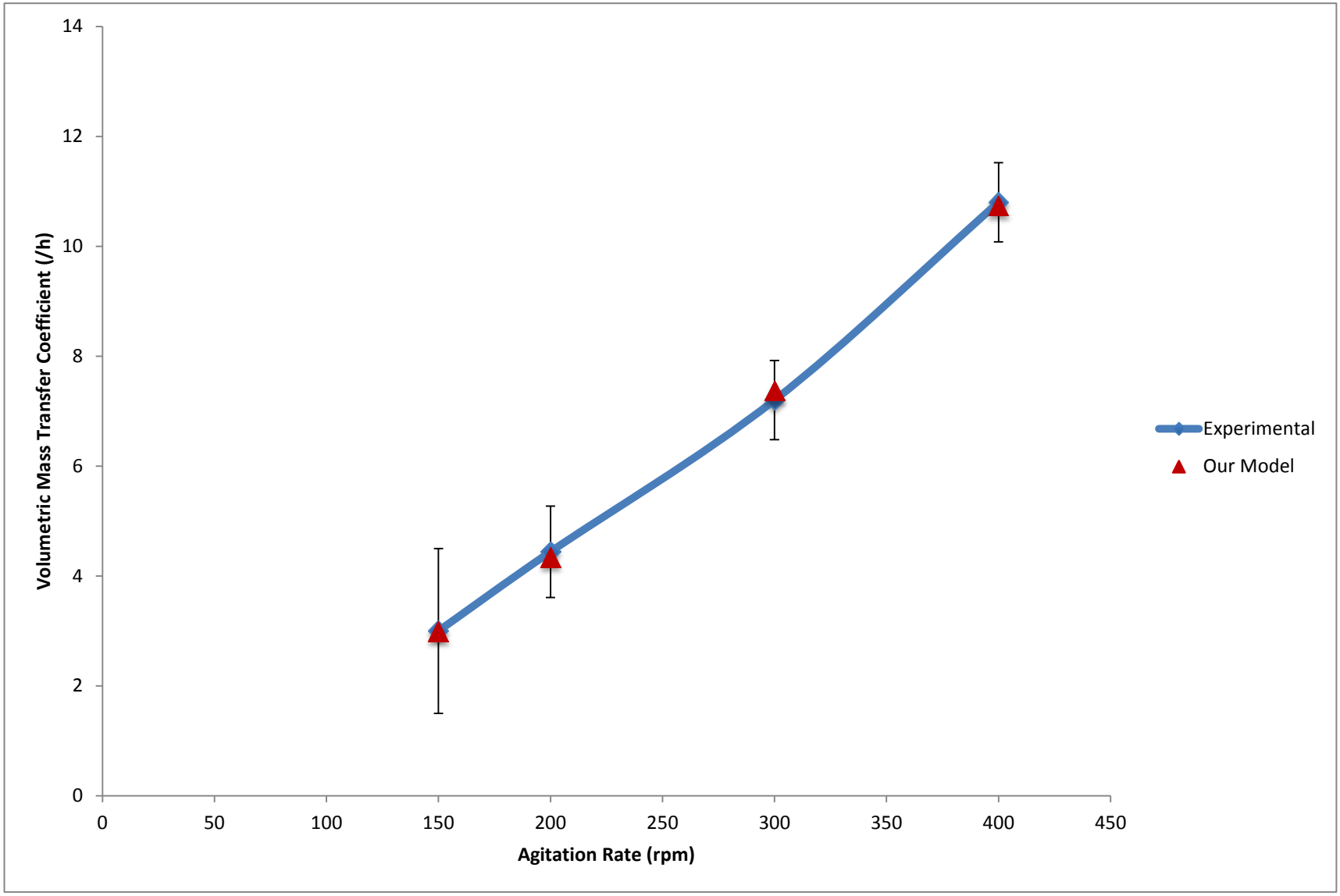

Figure 4.12: Comparison of the Experimental Results with the Calculated Data for 3% Carbon Dioxide at 1100 ml/min

In Figure 4.12 the blue line refers to the experimental results, whereas the maroon points are the results calculated using Equation 4.16. It can be seen in the figure that the correlation developed for K_La of CO_2 at 1100 ml/min is very accurate as the results obtained through it are strongly in accordance with the experimental results. Besides, having modeled K_La data points from Equation 4.16 within the error bars confirm the validity of the developed correlation. Thus, the Equations 4.16 can be used to directly calculate the volumetric mass transfer coefficient of CO_2 (3% in air) at the flowrate of 1100 ml/min and agitation rates from 150-400 rpm.

Similarly, Figures 4.13, 4.14 and 4.15 illustrate the accuracy of Equation 4.17 to determine the volumetric mass transfer coefficient of carbon dioxide at the gas flowrates of 2000, 2900 and 3500 ml/min and agitation rates from 150 to 400 rpm. The calculated values of K_La are very similar to the experimental K_La as all the data points in the graphs below are very close to each other and are within the error bars. Thus, it can be concluded that Equation 4.17 can accurately determine K_La of 3% CO_2 in air ranging at the flowrates ranging from 2000 to 3500 ml/min and agitation rates from 150-400 rpm.

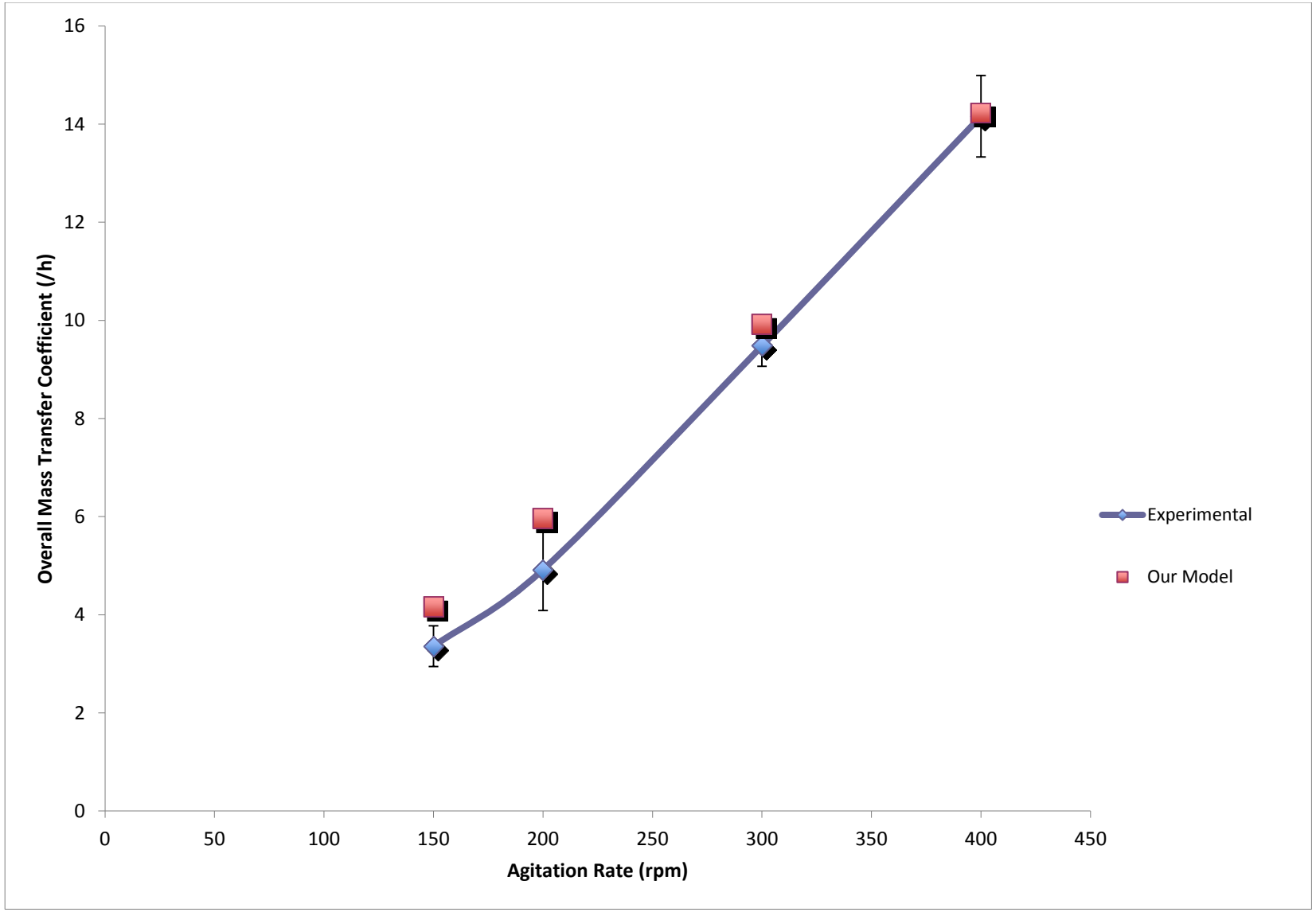

Figure 4.13: Comparison of the Experimental Results with the Calculated Data for 3% Carbon Dioxide at 2000 ml/min

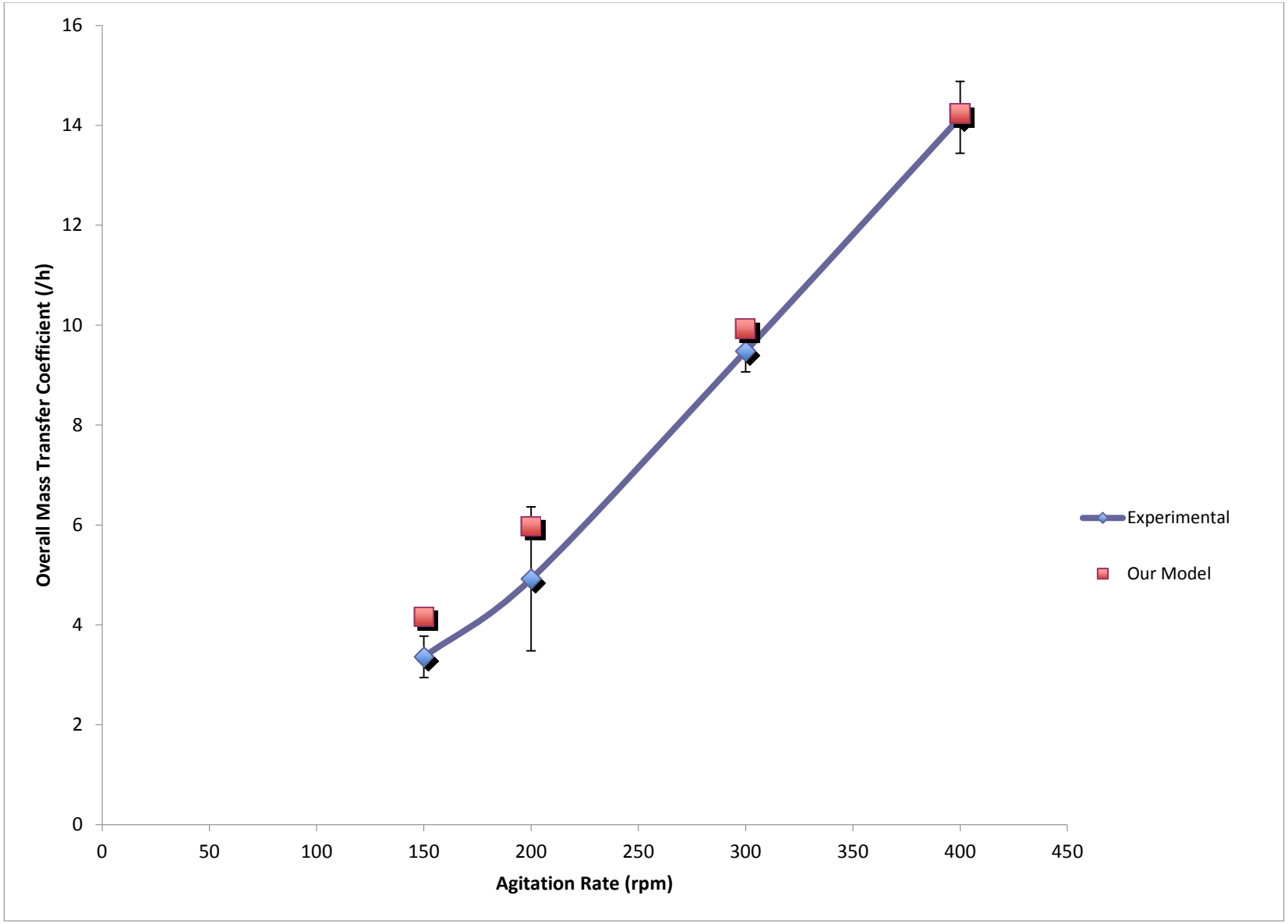

Figure 4.14: Comparison of the Experimental Results with the Calculated Data for 3% Carbon Dioxide at 2900 ml/min

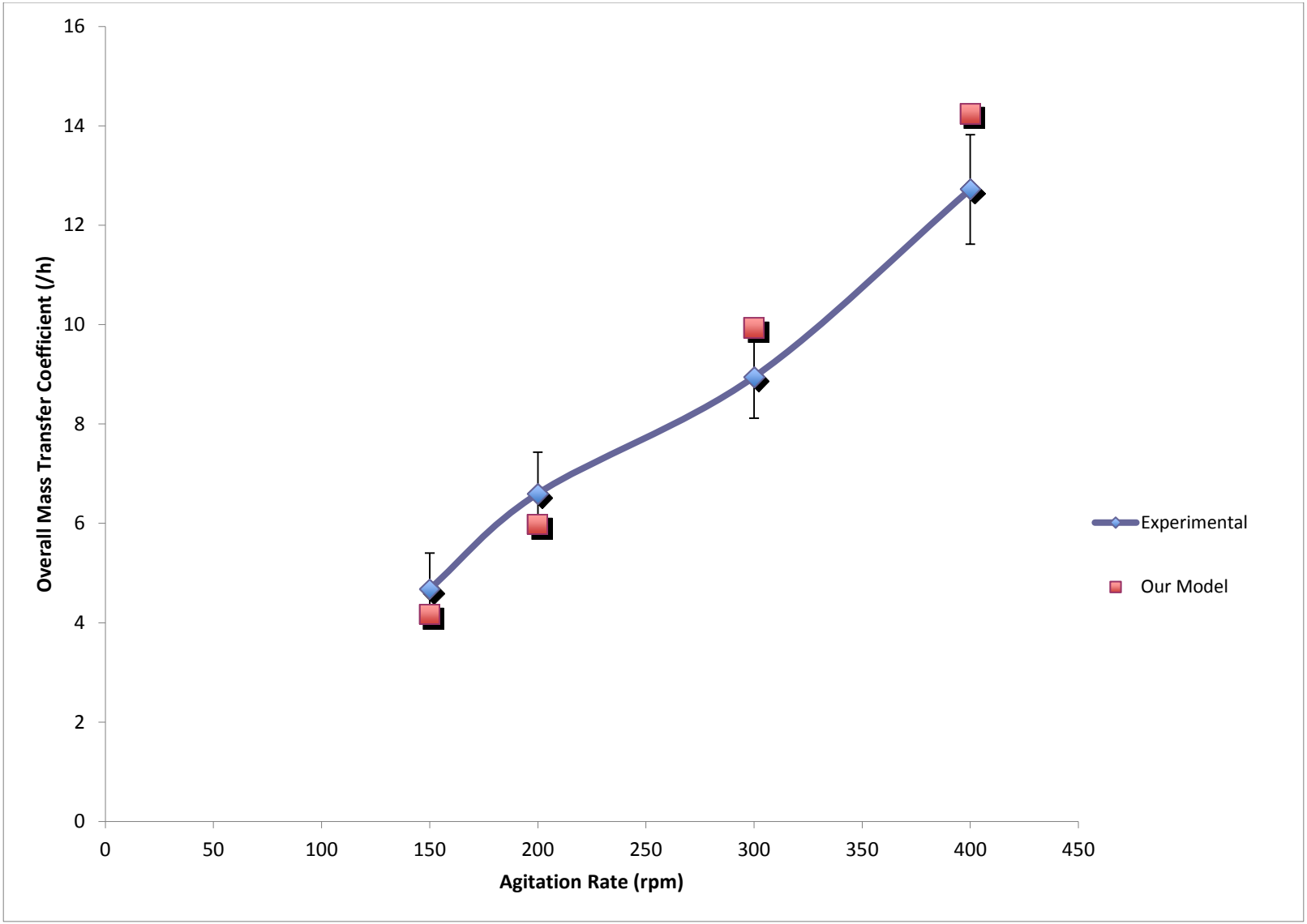

Figure 4.15: Comparison of the Experimental Results with the Calculated Data for 3% Carbon Dioxide at 3500 ml/min

Chapter 5: Conclusions and Recommendations

There were two key contributions in this study: Experimental protocols to measure the overall volumetric mass transfer coefficient of carbon dioxide $(K_La)_{CO2}$ in a stirred tank bioreactor , and theoretical correlations to calculate $(K_La)_{CO2}$ directly as a function of applied power were developed.

The results obtained from the experiment showed a direct relationship between the K_La of CO_2 and each individual parameter: agitation rate and gas flowrate (3% CO_2 in air). However, in the case of both parameters considered simultaneously a "Threshold Point" was observed at the agitation rate of 300 rpm and 2000 ml/min. At this point, an increase in the gas flowrate was making no difference in the K_La of CO_2. However, this "Threshold Point" was crossed upon increasing the agitation rate from 300 rpm to 400 rpm. The highest K_La value was observed at the gas flowrate of 2000 ml/min and agitation rate of 400 rpm. But, as the gas flowrate was increased beyond 2000 ml/min at 400 rpm a decrease in the K_La of CO_2 was observed.

The reason for this decrease can be explained due to the increased gas hold up and turbulence caused in the system because of higher gas flowrates and agitation rate. Under such a condition excessive presence of extremely small gas bubbles were formed which did not participate in the mass transfer of the gas to the liquid phase. Therefore, when the system was highly turbulent there was more gas hold up that led to the reduction in the K_La values.

Based on the K_La that was determined experimentally at various gas-flow and agitation rates, two theoritical correlations were developed to directly calculate the K_La of CO_2 inside a stirred tank bioreactor. The first correlation is applicable to the stirred tank vessels with a six-bladed dual Rushton Turbine operating at a lower flowrate of 1100 ml/min and agitation rates in the range of 150-400 rpm. Whereas, the second correlation can be used in stirred tank vessels operating at the gas flowrates from 2000 to 3500 ml/min and agitation rates from 150 to 4000 rpm. At a lower gas flowrate of 1100 ml/min, the superficial velocity (U_g) as well as gas hold up were small, therefore, the effect of superficial gas velocity (U_{gs}) on the K_La became negligible.

On the other hand, at the gas flowrates above 1100 ml/min, there was more gas hold up and higher superficial verlocity in the system, which made the effect of superficial gas velocity on the K_La more significant.

For this reason, two separate theoretical correlations were developed to determine K_La of CO_2: First correlation was for the gas flowrate of 1100 ml/min at the agitation rates from 150-400 rpm, and the second correlation was for gas flowrates ranging from 2000 ml/min and 3500 ml/min at the agitation rates from 150-400 rpm.

The direct method employed in this experiment was an efficient way of measuring the concentration of dissolved carbon dioxide. There were no complex calculations involved to determine the overall volumetric mass transfer coefficient of carbon dioxide. In addition, it proved to be a robust probe as it could handle turbulent conditions without showing fluctuations in the readings, and did not wear off. Therefore, the carbon dioxide ion selective electrode is recommended to directly measure the concentration of dissolved carbon dioxide, and thus the overall mass transfer coefficient of carbon dioxide inside stirred tank vessels in fermentation processes.

Moreover, the K_La correlations developed through the methodology employed in this study are very useful to determine the overall mass transfer coefficient of carbon dioxide in fermentation broths. The information about K_La of CO_2 plays a key role to quantify the carbon dioxide absorption by cell cultures. Hence, using the developed K_La correlations to quantify the carbon dioxide absorption by microalgae can overcome the challenge of desigining the photobioreactors with maximum CO_2 transfer into microalgae. Furthermore, the determined combination of agitation rate and the gas flowrate for 3% CO_2 in air for enhanced K_La of CO_2 was proved to be applicable for enhanced cultivation of microalgae inside the stirred tank bioreactor. As a result, it is possible to grow microalgae in excess inside the stirred tank vessels using the same combination of operating parameters as reported in this work. Thus, the proposed K_La correlations in this work, and combination of operating parameters for a stirred tank bioreactor to grow microalgae can bring an industrial revolution in the fields of biofuels, cosmetics and food.

Future Work:

The power P in the correlations developed to calculate K_La of CO_2 was calculated by assuming both upper and lower impellers in the turbine to be under flooding-loading transition. Therefore, the extent to which the results may vary upon applying the correlations in the case of stirred tank vessels with a single impeller is not known. However, this can be investigated in the future work. Also, in future the correlation developed for the gas flowrates from 2000 ml/min and 3500 ml/min can be investigated for the gas flowrates above 3500 ml/min. Based on the observations from this study, it could be possible that the correlation may be applicable in the stirred tank bioreactors with high gas flowrates. In addition, the same experiment as in this study can be repeated by growing microalgal cells in a liquid volume of 10L to have both impellers contributing towards agitation. This will provide the information about the survival of microalgal cells with dual impeller turbines running at high agitation rates. Further, correlations for the K_La of CO_2 in stirred tank vessels with microalgae in them can be developed.

Also, the methodology employed in this work to determine the concentration of dissolved carbon dioxide can be used to cultivate microalgae in bubble columns operating under various operating conditions. In this way, it will be possible to find out more about the limitations and flexibility of the CO_2 electrode.

Bibliography:

Alford Jr, J., 1976. Measurement of dissolved carbon dioxide, Canadian journal of microbiology 22(1), 52-56.

Andrew, S. P. S., 1982. Gas-Liquid Mass Transfer in Microbiological Reactors, Trans. IChe 60, 3-13.

Babcock, R. W., Malda, J., Radway, J. A. C., 2002. Hydrodynamics and mass transfer in a tubular airlift photobioreactor, Journal of Applied Phycology 14(3), 169-184.

Borkowski, M., 2005. Dissociation Constants, http://www.chembuddy.com/?left=BATE&right=dissociation_constants 2012(08/22).

Cents, A. H. G., 2003. Mass Transfer and Hydrodynamics in Stirred Gas-Liquid-Liquid Contactors. : University of Twente.

Chisti, Y., 2007. Biodiesel from microalgae, Biotechnology Advances 25(3), 294-306.

Doran, P. M., 1995. Mass Transfer, in: Anonymous Bioprocess Engineering Priniciples, pp. 190.

Doucha, J., Straka, F., Lívanský, K., 2005. Utilization of flue gas for cultivation of microalgae *Chlorella sp*. in an outdoor open thin-layer photobioreactor, Journal of Applied Phycology 17(5), 403-412.

Eucken, Grutzner, J., 1927. Journal of Physical Chemistr 125(363).

Farajzadeh, R., Barati, A., Delil, H. A., Bruining, J., Zitha, P. L. J., 2007. Mass transfer of CO2 into water and surfactant solutions, Petroleum Science and Technology 25(12), 1493-1511.

Farajzadeh, R., Zitha, P. L. J., Bruining, J., 2009. Enhanced mass transfer of CO2 into water: experiment and modeling, Industrial & Engineering Chemistry Research 48(13), 6423-6431.

Fisher Scientific Company, 2007. Instruction Manual XL Comm Data Acquisition Software for XL Series Meters. Ottawa: Fisher Scientific Company.

Hatta, J., 1929. Society of Chemical Industry. 32(809).

Hill, G. A., 2006. Measurement of overall volumetric mass transfer coefficients for carbon dioxide in a well-mixed reactor using a pH probe, Industrial & Engineering Chemistry Research 45(16), 5796-5800.

Johnson, M. S., Billett, M. F., Dinsmore, K. J., Wallin, M., Dyson, K. E., Jassal, R. S., 2010. Direct and continuous measurement of dissolved carbon dioxide in freshwater aquatic systems—method and applications, Ecohydrology 3(1), 68-78.

Kordac, M., Linek, V., 2008. Dynamic Measurement of Carbon Dioxide Volumetric Mass Transfer Coefficient in a Well-Mixed Reactor Using a pH Probe: Analysis of the Salt and Supersaturation Effects, Industrial & Engineering Chemistry Research 47(4), 1310-1317.

Kratena, J., Fort, I., Bruha, O., 2001. Dynamic Effect of Discharge Flow of a Rushton Turbine Impeller on a Radial Baffle, Acta Polytechnica 41(1).

Livansky, K., 1993. Dependence of the Apparent CO_2 Mass Transfer Coefficient K_La on the Nutrient Solution pH in Outdoor Algal Culture Units, Algological Studies 71 , 111-119.

Lydersen, B. K., Delia, N. A., Nelson, K. L. (Eds), , 1994. Bioprocess Engineering: Systems, Equipment and Facilities. USA: John Wiley & Sons, Inc.

Nedeltchev, S., Jordan, U., Schumpe, A., 2006. A new correction factor for theoretical prediction of mass transfer coefficients in bubble columns, Journal of Chemical Engineering of Japan 39(12), 1237-1242.

New Brunswick Scientific Company, 2009. Guide to Operations: Biocommand Tranck & Trend and Batch Control Bioprocessing Software. New Jersey: New Brunswick Scientific Company.

Omega Engineering Inc., 1992. ISE-8750: Carbon Dioxide Gas-Sensing Electrodes. USA: Omega Engineering Inc.

Payne, J. W., Dodge, B. F., 1932. Rate of Absorption of Carbon Dioxide in Water and in Alkaline Media, Industrial & Engineering Chemistry 24(6), 630-637.

Royce, P. N. C., Thornhill, N. F., 1991. Estimation of dissolved carbon dioxide concentrations in aerobic fermentations, AICHE Journal 37(11), 1680-1686.

Ryu, H. J., Oh, K. K., Kim, Y. S., 2009. Optimization of the influential factors for the improvement of CO2 utilization efficiency and CO2 mass transfer rate, Journal of Industrial and engineering chemistry 15(4), 471-475.

Sherwood, T. K., Pigford, R. L., Wilke, C. R., 1975. Mass Transfer. New York: McGraw-Hill.

Singh, M. K., Majumder, S. K., 2010. Theoretical Studies on Effect of Operating Parameters on Mass Transfer in Bubbly Flow, Journal of Engineering and Applied Sciences 5(2), 160-173.

St-Pierre, A., 2008. Measuring Greenhouse Gases in Aquatic Environments, EASTMAIN EM-1 2012(May 26), 4.

Taghavi, M., Zadghaffari, R., Moghaddas, J., Moghaddas, Y., 2011. Experimental and CFD investigation of power consumption in a dual Rushton turbine stirred tank, Chemical Engineering Research and Design 89(3), 280-290.

The Engineering Toolbox, Soubility of Gases in Water, http://www.engineeringtoolbox.com/gases-solubility-water-d_1148.html 2012(08/22).

TK Ghosh, T. K. G., Debnath Bhattacharyya, D. B., Tai-hoon Kim, T. K., 2010. Effect of Fractional Gas hold-up (εG) on Volumetric Mass Transfer Co-efficient (KLa) in Modified Airlift Contactor, International Journal of Advanced Science and Technology 16, 21-30.

Treybal, R. E., 1968. Mass-Transfer Operations. Tokyo: McGraw-Hill.

Weiss, R. F., 1974. Carbon dioxide in water and seawater: the solubility of a non-ideal gas, Marine Chemistry 2(3), 203-215.

Wilhelm, E., Battino, R., Wilcock, R. J., 1977. Low-pressure solubility of gases in liquid water, Chemical reviews 77(2), 219-262.

Yeh, S. Y., Peterson, R. E., 1964. Solubility of carbon dioxide, krypton, and xenon in aqueous solution, Journal of pharmaceutical sciences 53(7), 822-824.

Appendix-I

Theory of Operation of the Carbon Dioxide Probe:

The carbon dioxide probe has an ion selective membrane that allows the passage of dissolved carbon dioxide. Dissolved CO_2 in the sample solution continues to pass through the membrane until equilibrium between the partial pressures of CO_2 in the sample solution and refill solution inside the electrode is reached. Once the CO_2 diffuses through the membrane there is a change in the concentration of H^+ ions of the refill solution as shown in the following equation.

$$CO_2 + H_2O \rightarrow H^+ + HCO_3^- \quad (1)$$

The following equation relates the hydrogen ion, bicarbonate ion, carbon dioxide and water:

$$\frac{[H^+][HCO_3^-]}{[CO_2]} = Constant \quad (2)$$

The bicarbonate ion in the above equation can be assumed as constant due to the excessive quantity of sodium bicarbonate present in the refill solution. Thus, the above equation can be written as follows:

$$[H^+] = [CO_2]x\ Constant \quad (3)$$

The relationship between the potential of the pH sensing element and the hydrogen ion concentration is expressed using the Nernst equation:

$$E_o = E_1 + S\log[H^+] \quad (4)$$

Where,

E = Measured electrode potential

E_o = Reference potential (a constant)

$[H^+]$ = Hydrogen ion concentration

S = Electrode slope

Since the hydrogen ion concentration is directly related to the carbon dioxide concentration, electrode response to carbon dioxide is also Nernstian:

$$E_o = E_1 + S \log[CO_2] \quad (5)$$

Where, E_1 is the reference potential partly determined by the internal reference element that responds to the fixed level of chloride in the internal filling solution.

The amount of carbonate and biocarbonate ions is dependent on the pH of the solution. Therefore, the pH of the solutions is kept between 4.5 and 5 as all the carbonate and bicarbonate ions convert to dissolved carbon dioxide at within this pH range.

Figures of the Equipment:

Carbon Dioxide Probe

Bioreactor

Curriculum Vitae

Name:	Syeda (Anam) Kazim
Education and Degrees	The University of Western Ontario, London, ON, Canada 2010-2012 M.E.Sc- Biochemical Engineering The University of Western Ontario, London, ON, Canada 2005-2009 B.E.Sc- Chemical Engineering
Certifications	Six Sigma Green Belt, Lean Management Certificate
Honours and Awards	Capstone Design Project Competition- 2nd Prize
Related Work Experience	Teaching Assistant The University of Western Ontario 2010-2011 Research Assistant The University of Western Ontario 2006-2007, 2007, 2009
Publication (s)	U.S. Patent Application: Gurski, S.M.,Kazim, A., Cheung, H.K, Obeid, A., (2010) System and Process of Biodiesel Production, (U.S. Patent 8,192,696)